

AN INVESTIGATION OF THE PERFORMANCE
OF AN AXIAL FLOW COMPRESSOR WITH
EMPHASIS ON THE EFFECT OF
REYNOLDS NUMBER

ROBERT L. HANSEN
CHARLES L. JOSLIN

Library
U. S. Naval Postgraduate School
Monterey, California

Book 22

3854

AN INVESTIGATION OF THE PERFORMANCE OF AN AXIAL
FLOW COMPRESSOR WITH EMPHASIS ON THE EFFECT OF REYNOLDS NUMBER

by

R. L. Hansen, LCDR, United States Navy
B.S.E.E., United States Naval Academy
1942

B.S.A.E., United States Naval Postgraduate School
1951

and

C. L. Joslin, Jr., LT., United States Navy
B.S. United States Naval Academy
1943

B.S.A.E. United States Naval Postgraduate School
1951

Submitted in Partial Fulfillment of the
Requirements for the Degree of
Master of Science
at the

Massachusetts Institute of Technology

May 16, 1952

M.I.T. Gas Turbine Laboratory
Cambridge 39, Massachusetts
May 16, 1952

Professor Shatswell Ober, Chairman,
Department Committee on Graduate Students
Department of Aeronautical Engineering
Massachusetts Institute of Technology
Cambridge 39, Massachusetts

Dear Sir:

In partial fulfillment of the requirements for the degree of Master of Science in Aeronautical Engineering, we hereby submit a thesis entitled "An Investigation of the Performance of an Axial Flow Compressor with Emphasis on the Effect of Reynolds Number".

Abstract

AN INVESTIGATION OF THE PERFORMANCE OF AN AXIAL
FLOW COMPRESSOR WITH EMPHASIS ON THE EFFECT OF REYNOLDS NUMBER

by

R. L. Hansen, LCDR, United States Navy
C. L. Joslin, Jr., LT., United States Navy

Submitted to the Department of Aeronautical Engineering on May 16,
1952, in partial fulfillment of the requirements for the degree
of Master of Science.

The performance of the compressor component of the Westinghouse X9.5B Turbo Jet Engine was investigated. This six-stage axial flow compressor was driven in a quasi closed air circuit by its own turbine and a supersonic wind tunnel air supply. The variation of the stage pressure rise with air flow and the effect of Reynolds number on the overall performance was studied. The Reynolds number chosen was one defined by the compressor rotor speed, blade chord, and inlet conditions. The investigation was conducted over a range of Reynolds numbers between 136,000 and 307,000 and compressor speeds generally lower than those used in normal operation. The test was prematurely brought to an end by the rupture of the turbine blading at 25,000 r.p.m. from an undetermined cause.

A stage by stage static pressure survey precisely demonstrated the qualitative explanation of the effect of mass flow on the stage performance. The data indicated that the reduction in compressor maximum efficiency at low Reynolds numbers was small. Trends of efficiency versus Reynolds numbers presented by the National Advisory Committee for Aeronautics were reproducible only if the proper pressure ratios were arbitrarily chosen. This was believed to be characteristic of the compressor tested and the operating range used. One suggested means of attempting verification of the assumption of Reynolds number as an important performance parameter was presented.

The investigation was conducted by the authors at the Gas Turbine Laboratory, Massachusetts Institute of Technology, Cambridge 39, Massachusetts, between September 1951 and May 1952.

Thesis Supervisor: Edward S. Taylor
Title: Professor of Aircraft Engines

Acknowledgements

The authors wish to express their gratitude to Professor Edward S. Taylor for his help and suggestions in the development of this investigation, and to the Staff of the Gas Turbine Laboratory for their cooperation and assistance.

Table of Contents

I	Abstract	Page
II	Introduction	1
III	Equipment and Procedure	6
IV	Results and Discussion	14
V	Conclusions	21
VI	Recommendations	23
VII	Appendices	
	Appendix A--Symbols	26
	Appendix B--Calculations	28
VIII	References	33
IX	Bibliography	34
X	Tables	
	Table I--Compressor Performance Data	35
	Table II--Survey of Static Pressures	37
	Table III--Summary of Dimensionless Performance Variables	39
XI	Figures	
	Figure 1--Cutaway View of Westinghouse X9.5B Turbo Jet Engine	41
	Figure 2--Exploded View of Test Compressor	42
	Figure 3--Arrangement of Compressor Test Stand	43
	Figure 4--Duplex Chamber, Schematic View of External Arrangement	44
	Figure 5--Duplex Chamber, Schematic View of Internal Arrangement	45
	Figure 6--Test Compressor Showing Inlet Arrangement and Measuring Stations	46

	Page
Figure 7--Instrumentation of Plenum Chamber at Inlet of Compressor	47
Figure 8--Instrumentation of Annular Outlet of Compressor	48
Figure 9--Details of Pressure Instrumentation	49
Figure 10--Details of Thermocouple Construction	50
Figure 11--Overall View of Compressor Test Set-Up	51
Figure 12--Intermediate View of Compressor Test Set-Up	52
Figure 13--Close-Up of Test Compressor	53
Figure 14--Compressor Performance Map of Various Inlet Densities	54-58
Figure 15--Manometer Board Showing Uniform Pressure Rise Near Surge Point	59
Figure 16--Manometer Board Showing Pressure Loss at High Mass Flow	60
Figure 17--Compressor Axial Pressure Distri- bution	61
Figure 18--Performance Map of Compressor at Various Mach Numbers	62-65
Figure 19--Variation of Maximum Compressor Efficiency with Reynolds Number	66
Figure 20--Variation of Compressor Efficiency with Reynolds Number at Several Pressure Ratios	67-68
Figure 21--Variation of Pressure Ratio for Maximum Efficiency with Reynolds Number	69

	Page
Figure 22--Effect of Compressor Inlet Reynolds Number on Compressor Efficiency (NACA RM E9G11)	70
Figure 23--Effect of Compressor Inlet Reynolds Number on Fraction of Rated Air Flow (NACA RM E9G11)	71

Introduction

This thesis is concerned with an experimental investigation of the compressor component of the Westinghouse X9.5B turbo-jet engine. Its purpose was to measure the performance of the compressor over the available range and to study the effects on performance caused by a variation in Reynolds number.

To those familiar with the gas turbine type of jet engine, it is well known that the accurate analysis or prediction of the performance of an axial flow compressor presents a difficult problem. This is particularly true for "off design" conditions of operation where the problem becomes, in fact, generally unsolved.

The known reasons for the deficiencies in the theory on the axial compressor are many. The inherent complexities of flow through a stage of stationary and rotating blades, familiar to the turbine experts, is further complicated in the compressor by the interaction effects of all the other stages present and the basic aerodynamic difference between a diffusing flow and one which accelerates.

Following turbine practice, present methods of axial compressor analysis apply the available flow theory to a series of stage by stage computations incorporating corrections based upon experimental data usually obtained from wind tunnel tests on stationary cascades.

Since a specific complete calculation applies to only one operating condition, the enormous amount of work then necessary in order to predict the characteristics over a wide operating range is immediately apparent. Add to this the fact that agreement of theoretical calculations with actual performance is usually not too close, and a strong argument is presented for a simpler method of performance prediction for the axial compressor designer.

The most logical possibility would seem to be a more or less empirical prediction procedure drawn from a large fund of performance data on previous models. It is probable that initial stage by stage computations must be made, however, it is possible that the variation in performance from the design condition may be obtained with reasonable accuracy from experimental relations, including correlation with geometrically similar models. For such a system, however, it is first necessary that the variables affecting performance be recognized and their effects determined. For this reason, the primary object of this thesis was to investigate the variation in performance of the Westinghouse compressor with Reynolds number.

In the study of airfoil characteristics at subcritical Mach numbers, the Reynolds number is the important similitude parameter permitting comparison or prediction of lift and drag coefficients for airfoils and even airplanes of the

same aerodynamic shape. For this use, each term of the Reynolds number has an accepted definition and its effect is related to the transition point and the shifting of the separation region on the airfoil. If the airfoil is used in a cascade, these characteristic variations with Reynolds number may be correlated directly with the cascade efficiency and corrected air flow.

Because of this, in an axial flow compressor investigation made by the NACA, Ref. (a), a compressor-inlet Reynolds number was defined as:

$$Re = \frac{c \rho_3 V_{3,r}}{\mu_3}$$

where, c = chord length of first-stage rotor blade measured midway between blade root and tip, ft

ρ_3 = density of air at inlet to first rotor stage, slugs/cu.ft.

$V_{3,r}$ = velocity at inlet to first rotor stage relative to rotor blades, ft/sec

μ_3 = viscosity of air at inlet to first rotor stage, lb-sec/sq.ft.

For the first rotor stage of the compressor, this corresponds to the accepted airfoil Reynolds number.

In this thesis, the approach to the Reynolds number effect was somewhat different. The performance of an axial compressor is normally presented graphically in two coordinates. At a

fixed inlet density, the pressure ratio and/or efficiency is usually plotted versus corrected mass flow, with corrected engine speed as a parameter. Other equivalents of the mass flow and corrected speed are sometimes used. Inclusion of the Reynolds number into the function of either of these four variables introduces the effect of viscosity on the performance.

Since the Reynolds number contains a density term and in order not to introduce a new parameter into the picture, it was decided to attempt description of the performance by the four dimensionless variables; compressor pressure ratio, corrected mass flow expressed as a fraction of sea level rated air flow, compressor Mach number, and Reynolds number. Such a choice of variables cannot be an arbitrary one, and the first requirement to be met as to their suitability is that any one of them be uniquely determined when the other three are fixed. The added requirement of dimensional consistency is also met by the selected parameters.

As noted, the usual concept of the Reynolds number for an axial compressor is the airfoil Reynolds number applied to one of the blades. Unfortunately, such a Reynolds number is extremely difficult to compute or obtain for application to ordinary compressor operation, and there is, of course, a different such Reynolds number for each row of blades in the compressor.

On the other hand, the four terms of the Reynolds number

may be defined in such a manner that the combination is readily obtainable and will still meet the initial requirement of dependence upon the other performance parameters. The complexity of the function relating the variables is not, of course, independent of this choice of form.

However, in view of the practical advantage to engineers of an easily calculated Reynolds number as opposed to the airfoil Reynolds number applied to a compressor, the definition which was decided upon for this investigation was:

$$Re = \frac{\rho_{01} u c}{\mu_{01}}$$

where ρ_{01} = total density of air at compressor inlet,
lbs/ft³

u = compressor tip speed, ft/sec.

c = mean chord length of first stage rotor blades,
ft.

μ_{01} = total viscosity of air at compressor inlet,
lbs/sec.ft.

It should be emphasized that, in the absence of strong evidence to the contrary, any specific variation in the overall performance of a compressor with the Reynolds number could be expected to apply at most to a series of geometrically similar models. On the other hand, certain trends in the performance caused by Reynolds number variation may well have general application.

Equipment and Procedure

The compressor tested was a component of the Westinghouse Model X9.5B Turbojet Engine. It is a six stage, eight inch diameter axial flow compressor with a nominal pressure ratio of three and a rated air flow of 6.8 pounds per second under static conditions at sea level. The normal r.p.m. is 31,200. A cutaway view of the original engine is presented as Figure 1, and a photograph of the disassembled compressor as Figure 2. Further detailed information is available in Reference (b).

The investigation utilized a compressor test stand designed in conjunction with and described in Reference (c). The stand was modified as described below to overcome difficulties noted in Reference (c) and to provide the more thorough instrumentation desired. The design of the test setup, a sketch of which is presented in Figure 3, included a modification of the original turbo compressor unit permitting the turbine to be driven by the supersonic wind tunnel air supply while the compressor operated in a quasi closed air circuit. Thus, the test unit consisted of two distinct air circuits--the power air circuit, driving the turbine, and the compressor air circuit. This arrangement allowed concurrent investigation of both the compressor and the turbine performance, the latter being the subject of another thesis.

As noted in Reference (c), in order to provide the two

separate air circuits, it was necessary to modify the original combustion chamber by inserting a partition, thus forming a turbine inlet space on one side and a compressor outlet connection on the other. This section was known as the duplex chamber. It will be noted (Figures 4 and 5) that the rubber diaphragm forming the partition, as described in Reference (c), was replaced by a metal one as recommended therein.

A further alteration of the engine involved modification of the lubrication system. The modification was necessary to prevent oil from being exhausted into the wind tunnel through the turbine outlet connection. Briefly, it consisted of: (1) moving the oil mist nozzle from the front to the rear of number three bearing, (2) providing a pressurized gland about the turbine shaft to the rear of the bearing, and (3) connecting the laboratory steam ejector through an oil trap to the combustion chamber inner casing in front of the bearing. Thus the oil mist presumably traveled from the rear of number three bearing, as well as from the front of number two bearing, through the bearings, into the combustion chamber inner casing, hence out of the engine to the oil trap. In addition to the above, the authors decided to connect the laboratory ejector to the accessory drive gear box through an available passage in the support struts. (See Reference (b)). This was done in the hope of minimizing the flow of oil through the compressor, such flow being a feature of the original design. Neither of these modifications was

completely effective. Although most of the oil was properly ejected, an excessive amount entered both the wind tunnel and the compressor air circuit. (See Recommendations). The air supply to the oil mist mixer was obtained from a separate compressed air supply connected to the mixer through a regulator. The supply pressure was maintained at twenty-six pounds per square inch, gauge.

As noted previously, the setup consisted of two separate air circuits. In the power air circuit, the air flowed from the wind tunnel outlet valve, through twelve inch ducting, a transition member narrowing to eight inch piping, thence into the turbine side of the duplex chamber. The air then expanded through the turbine and exhausted through another transition member to the wind tunnel inlet valve. The power output of the turbine was controlled by varying the air flow through the wind tunnel system and adjusting the inlet and outlet pressures.

In the compressor air circuit, the compressor exhausted into one side of the duplex chamber, thence through a system of piping to a gate valve. The valve provided the necessary control of air flow through the compressor. On the opposite side of the gate valve, a 3/4 inch connection was made to the laboratory steam ejector. Adjacent to this connection was a small bleed valve whereby air from the atmosphere could be bled into the circuit. The adjustment of these devices was intended to provide the desired degree of flexibility in the compressor inlet pressure. From this point air passed through ten inch

pipng to a transition flange, and through a twenty-four inch elbow provided with vertical guide vanes to two air coolers. The coolers, being tubular, cross flow heat exchangers, served the dual purpose of providing temperature control and straightening of the air flow to the compressor. From the coolers the air flowed through the plenum chamber, which contained an additional wire screen straightener, and finally through a calibrated nozzle to the compressor inlet duct. It was found during the first group of runs that the bleed valve described above was of insufficient size to allow operating at atmospheric inlet pressures. This deficiency was remedied by installation of a three inch valve to the atmosphere at the bend adjacent to the transition flange. The alteration is indicated by broken lines in Figure 3. In addition, response of the inlet pressure to the suction of the ejector was somewhat slower than desired. (See Recommendations).

The plenum chamber and compressor inlet conform to the general specifications outlined in Reference (d). The wooden nozzle had been calibrated against a standard orifice for air flow measurement and the calibration data presented in Reference (c). The mounting of the nozzle on the plenum chamber (previously by means of a rubber diaphragm) and the attachment of the compressor thereto were redesigned. The new arrangement may be seen in Figure 6.

The instrumentation of the test setup is illustrated by

Figures 6 to 10. That installed at stations (0) and (2) is substantially as recommended by Reference (d). In the plenum chamber, station (0), two static pressure taps, two total pressure rakes (three tubes each) and six thermocouples were installed as shown. The total pressure probes and thermocouples were all arranged symmetrically at area centers of equal areas. In the compressor outlet, station (2), four static pressure taps, four thermocouples and one total pressure tube were installed as shown. In addition, in order to utilize the calibrated nozzle for air flow measurement, three static pressure taps were placed in the compressor inlet, station (1), one of the stations used during calibration. As a matter of additional interest, it was decided to obtain the axial pressure distribution within the compressor by placing static pressure taps at each row of stator and rotor blades. These stations are illustrated in Figure 6. The instruments were installed in the manner shown in Figures 9 and 10, the pressure taps being 0.030" diameter holes with take-offs of 1/8" steel tubing, press fitted as shown. The thermocouples were substantially similar to those recommended in Reference (d). The pressure taps and total pressure tubes were connected through plastic tubing to a mercury manometer board. A differential water manometer was also connected to stations (0) and (1) in order to read the pressure drop across the calibrated nozzle essential to air flow determination.

Thermocouples were connected through selector switches to a potentiometer and referred to a common ice point as recommended in Reference (e). The temperatures of the three bearings were read by means of the installed bearing thermocouples and standard aircraft cylinder head temperature gages, while the r.p.m. were obtained through use of the installed tachometer generator and a standard aircraft tachometer. Photographs of the complete installation are presented as Figures 11 to 13.

The laboratory procedure followed is of interest primarily due to the problems encountered. Initial and periodic tests were made for leakage in the system, including manometer connections, by placing the compressor air circuit under a static vacuum. Thermocouples were checked against room temperature daily, prior to beginning the runs. The first thirty-two runs were exploratory in nature, and were made at controlled engine speeds only, the inlet density and the mass flow at selected speeds being varied as widely as practicable by the three controls in the compressor air circuit. In this manner it was intended that the limits of operation be determined and a skeleton set of data be obtained about which to build a coordinated investigation.

As mentioned previously the speed of the turbo compressor was controlled by the regulation of the airflow through the wind tunnel system and through adjustment of the turbine

inlet and outlet densities. The speed was, of course, a function not only of the wind tunnel control but also of the load on the compressor. Furthermore, the inlet pressure was influenced by the r.p.m. and compressor air flow. Consequently, accurate control of the variables involved became a somewhat delicate problem, necessitating trial and error adjustments with sufficient time at each setting to allow the attainment of equilibrium in the circuit. It was found after installation of the three-inch bleed valve, previously mentioned, that the inlet pressure could be effectively varied between atmospheric and approximately six pounds per square inch, absolute, depending upon the compressor operating conditions. The lowest pressure that could be maintained regardless of compressor operating conditions was about eight pounds per square inch. This limitation was imposed primarily by leakage in the system and could have been lowered if warranted.

The inlet temperature was subject to variation by changing the rate of water flow through the coolers, but the control was unwieldy. The process was one of trial and error and the time required to reach equilibrium after adjustment was prohibitive. Introduction of variation in temperature distribution in the plenum chamber was noted upon changing the rate of water flow. This was, in all probability, due to variations in water distribution within the coolers. The most satisfactory conditions were obtained by operating the coolers at maximum capacity. The temperature

distribution, while not uniform, was considered to be adequately so.

Following the initial thirty-two runs during which the above information was gathered, succeeding tests were made at controlled inlet conditions, air flow, and engine speeds to fill out performance maps over the greatest possible range. Generally, data was taken at constant speed and inlet pressure at four different values of air flow, the lower limit being the surge point and the upper limit the maximum flow obtainable. It was intended that a performance map be found covering the chosen engine speeds at four distinct inlet pressures. It was anticipated that at least one hundred data runs would be required. In order to forestall possible bearing failure, it was decided to avoid high speed until a reasonable amount of data had been gathered in the lower speed range.

This procedure was completed in varying degrees at each of several engine r.p.m.'s, namely, 15,000, 16,000, 18,000, 20,000, 22,000, and 25,000.

Unfortunately, complete failure of the turbine was experienced after the fiftieth test run, and the entire desired coverage was not attained. The cause of the turbine failure was not determined, but while running at 25,000 r.p.m. the entire set of nozzle blades was suddenly torn out and carried through the turbine rotor, cutting each rotor blade in half. It would seem probable that such a failure could

only be caused by the passage of a solid particle through the turbine or by the initial displacement of a single nozzle blade into the rotor due to a critical stress condition. In any event the damage was irreparable in the time remaining to complete the thesis, and the investigation was limited to the fifty runs accomplished.

Results and Discussion

Following the procedure outlined above, the data obtained for each run consisted of: (1) engine speed, (2) temperature at the inlet and outlet, (3) the static pressure at the inlet, outlet, and at each row of blades, (4) the total pressure at the inlet, and (5) the pressure drop across the entrance nozzle. The method used to calculate the performance was straightforward and is described in detail in Appendix B. It should be noted that, in accordance with the recommendation in Reference (d), the total pressure at the outlet was calculated from the known mass flow, area, indicated temperature, and static pressure. The single total head tube placed in the outlet constituted a check on these calculations, and agreement was reasonably close throughout the tests.

A complete compilation of the results is given in Tables I and II. For convenience, a relisting of the five dimensionless performance parameters for each run has been included as Table III. Graphical presentations of the performance and its variation with Reynolds number are shown in Figures 14 through 21.

With the exception of two improbable efficiencies, at the lower pressures, the results were reasonable and apparently quite reproducible. The normal performance plots of pressure ratio and efficiency versus corrected fraction of rated air flow at constant inlet density with compressor

Mach number as a parameter are shown in Figures 14a to 14e. The maximum density which could be consistently maintained was 0.0726 lb/ft^3 which was very near to laboratory atmospheric conditions. Although the efficiency curves for the higher compressor Mach numbers were not obtained, it is probable that the efficiencies shown are representative of the entire operating range. It can be seen that an average maximum efficiency of approximately seventy-nine percent was consistently maintained. The increasing steepness of the curves of pressure ratio versus corrected fraction of rated mass flow, as the compressor Mach number was increased, is in agreement with axial compressor theory. Examination of these curves reveals that the "choke point" was never reached, since at a given Mach number and inlet density, variation in corrected air flow was always possible.

Throughout the investigation, the picture of the compressor performance given by the large manometer board was of considerable interest. The change in the velocity triangles for each row of blades in the compressor with a small variation in inlet conditions is extremely tedious to calculate and present here. However, it may be shown qualitatively that at a given speed an increase in mass flow will cause a progressive decrease in stage pressure rise. This decrease is due, in general, to the modification of the velocity diagram by an increase in axial velocity. Consider

the compressor to be operating at the normal operating condition defined by an approximately equal pressure rise per stage. Increase the mass flow. Then the axial velocity of the first stage will increase and the pressure rise in that stage will decrease. In the second stage the axial velocity will be increased not only by virtue of the greater mass flow, acting directly through the continuity equation, but also by the lower density of the air delivered by the first stage. In this manner the effect of an increase in mass flow is compounded throughout the compressor. If the increase were sufficiently large, as one proceeds axially through the compressor a stage will be reached which will give no pressure rise at all and later stages will actually show a pressure drop. Reference to the velocity diagram of one of these latter stages would reveal that it is operating as a turbine stage. Proceeding further toward the outlet one reaches the final stator stages and the diffuser where the pressure again increases progressively toward the outlet. Now suppose that, operating at normal conditions, the mass flow had been decreased instead of increased. The effect would have been in the opposite direction, namely, toward an increased stage pressure ratio. However, the resulting increased turning angle would soon result in a stalled stage and a surging compressor.

The above tendencies were precisely demonstrated by the interstage pressure measurements. Two photographs are

presented of the manometer board during operation at the same speed. Pressure is positive downward in both cases and the inlet is on the right. Figure 15 shows the board with the compressor operating near the surge point. The uniform pressure distribution is evident. Figure 16 demonstrates the condition during maximum mass flow, with the consequent loss in pressure rise and the dip in the pressure curve near the compressor outlet. The static pressure survey for each run is contained in Table II. In order to show the progressive development of the trends mentioned above, the axial pressure distribution has been plotted for four values of mass flow in Figure 17. As may be seen the trend is faithful to the theory. A progressive increase in mass flow caused a progressive decrease in pressure rise, noticeable mainly in the later stages. Due to the cumulative effect, a comparatively small mass flow increase caused a group of the later stages to exhibit the progressive pressure drop. This was invariably followed by a pressure rise in the final measuring stations due mainly to diffusing action.

A presentation of the variation of performance with Reynolds number is shown in Figures 18 through 21. The variation of compressor efficiency and pressure ratio with corrected fraction of rated air flow at constant Mach number with Reynolds number as a parameter is given in Figures 18a to 18d. It is of interest to note that in this presentation the compressor surge point for a given Mach number occurs at a

constant pressure ratio, regardless of Reynolds number. The normal performance plot of this compressor, on the other hand, shows a curved surge line.

It was expected that, at constant Mach number, a decrease in Reynolds number would result in a decrease in maximum compressor efficiency. This effect can be seen in the NACA investigation using the airfoil Reynolds number previously described. From the results of the subject test, however, the same conclusion cannot be definitely drawn, although the authors feel that substantiation has been made of the fact that the Reynolds number effect on maximum efficiency is a small one. In order to show this variation more clearly, a cross-plot of the maximum efficiency versus Reynolds number has been presented in Figure 19. Here it can be seen that at the highest compressor Mach number (0.658) a decrease in maximum efficiency of 0.03 occurred when the Reynolds number was decreased from 307,300 to 212,600. At the other Mach numbers the change was negligible. In view of the small changes involved, it is felt that a more exact quantitative description would require a large fund of experimental data, including repetitive runs.

In order to more completely show the relations among the different variables, Figures 20 and 21 have also been cross-plotted from the constant Mach number curves. Of these, Figures 20a and 20b show the effect of a variation in Reynolds number on the compressor efficiency at a given Mach number and

several values of compressor pressure ratio. These two figures are similar to the one given by the NACA, which is reproduced for comparison as Figure 22. By an arbitrary choice of pressure ratio a single figure could have been produced which would agree closely with the effect shown by the NACA. However, in Figures 20a and 20b, the effect of a change in pressure ratio is also included. It can be seen that the major trend is a decreasing efficiency with decreasing Reynolds number although the function is apparently complicated and the effect is again small. The curvature and reverse trend shown by the curves at certain pressure ratios reflect the greater variation of efficiency with pressure ratio of the Westinghouse compressor in the realm tested.

Figure 23 is a reproduction of a curve presented by the NACA. It is a plot of corrected fraction of rated mass flow versus Reynolds number at several pressure ratios and Mach numbers. Examination of the constant Mach number curves of this investigation reveals that the statements made above with regard to Figures 19 and 20 would apply equally well to this plot. In particular, the trend is a function of pressure ratio and for the compressor tested it could easily be reversed by the pressure ratio chosen. In addition, it is noted that the mass flow for maximum efficiency generally increases with Reynolds number.

The authors wish to emphasize that the tendencies

presented above might have been altered and in some cases even reversed had sufficient data been accumulated. The lack of such data drastically limited the ability to weed out possible bad points in the data plotted. It is considered particularly unfortunate that the realm closer to normal compressor speeds could not have been exhaustively investigated.

Finally, the thought occurs that, to date, no attempt known to the authors has been made to verify the assumption that Reynolds number is actually the optimum dimensionless parameter for the correlation of compressor performance in the manner described. Actually some other parameter involving density may be more appropriate. One procedure whereby an indication may be obtained of the value of Reynolds number in this respect is suggested under "Recommendations".

Conclusions

To the somewhat limited information available concerning the effect of Reynolds number on a complete axial flow compressor, further evidence has been added in this thesis as to the importance of this operating variable. Since in this investigation the effect was shown to be quite small, the relative error in numerical conclusions introduced by experimental procedure and the restricted scope of the test runs has been magnified. For this reason, the authors attach value to the qualitative rather than the quantitative results.

The effect of Reynolds number as a variable should become increasingly important in the low speed operating range of the compressor. Since this range was reasonably well covered, the small effects noted may be representative of the entire operating range:

The change in compressor efficiency and corrected mass flow caused by a change in Reynolds number is a function of the compressor Mach number and pressure ratio. At selected combinations of these latter parameters, a trend of decreasing efficiency and mass flow with decreasing Reynolds number can be shown. At other combinations, a reversed or curved trend is evident. In all cases, the effect is small. This statement applies also to the variation of maximum efficiency with Reynolds number at a given Mach number, the maximum change noted being a decrease of .03 in efficiency when

the Reynolds number decreased from 307,300 to 212,600.

For this compressor, the pressure ratio at which surge occurred was practically a function of compressor Mach number only and was apparently independent of Reynolds number and inlet pressure.

Recommendations

As brought out in the preceding discussion, the results obtained are not regarded as conclusive due to insufficient data. However, the lack of a positive trend within the operating range covered would seem to indicate that further investigation is unwarranted unless the operating range is considerably extended. Such extension should involve increasing the range of attainable compressor speeds and Reynolds numbers.

Consideration should be given to the feasibility of providing a power source other than the wind tunnel-turbine combination used. The maximum speed attainable at atmospheric inlet pressure was near 25,000 r.p.m. By reducing the inlet pressure to a very low value it would be possible to approach 31,200 r.p.m., the normal value for the subject compressor. However, such a procedure would almost entirely eliminate the range of variation of Reynolds number.

The range of Reynolds numbers may be increased sufficiently by (1) eliminating leakage in the system, both in the exterior fittings and between the compressor and turbine, and (2) by increasing the capacity of the ejector and bleed combination. It is likely that the three-inch bleed valve installed is of sufficient size to allow operation near atmospheric pressure with rated air flow, but the size of the ejector connection should be increased considerably to allow greater capacity and to cut down on the slow response of

inlet pressure to the suction of the ejector.

As noted under "Equipment and Procedure", the modification of the lubrication system was unsuccessful from the standpoint of preventing oil leakage into the wind tunnel system. Air leakage between the compressor and turbine also existed. A possible solution to the former may lie in the introduction of a more effective seal, probably of the labyrinth type, in back of number three bearing. The use of packing between the bearing and turbine may also be worth considering. Any other solution would involve relocation of the bearing with respect to the turbine, a doubtful procedure, at best. Leakage of oil and air between the compressor circuit and the turbine circuit would involve introduction of an effective seal between the last rotor stage and the compressor diffuser cone. Leakage from the bearing support assembly into the first compressor stage appears difficult if not impossible to eliminate without extensive redesign. The best overall solution appears to be to accept but minimize this latter leakage by balancing the oil mist flow entering the bearing support assembly with the capacity of the ejector suction fitting in that assembly. The compressor to turbine leakage may be entirely eliminated by cutting away an axial portion of the duplex chamber inner and outer casings, then inserting two partitions completely isolating

the compressor circuit from the turbine circuit. The bare drive shaft, possibly extended, would be the only connection between compressor and turbine.

The practicability of varying the inlet temperature sufficiently to allow operation at the same inlet density and Mach number but at different Reynolds numbers (varying viscosity) should be studied. For example, if the temperature could be varied from, say, 500°R to 650°R , the speed from 20,000 r.p.m. to 22,800 r.p.m. and the pressure from 11.3 to 14.7 psia, the Mach number and density would be constant while the Reynolds number would vary by a factor of $\mu_2/\mu_1 = 118/143 = 0.825$. Such a procedure, if it could be carried out over sufficient range, would provide one indication of the value of Reynolds number as a parameter. It would in essence indicate its sufficiency. Its necessity could be shown by varying the density but keeping Mach number and Reynolds number constant. The proposal would necessitate introduction of much better means of temperature control than currently exists in the apparatus in order to provide a significant range of investigation.

Finally, further tests will require recalibration of the air flow measuring nozzle. The data should be extended to include mass flows up to at least 6.8 lbm/sec for use with the subject compressor.

Appendix (A)

Symbols

A	Air flow area
H	Total enthalpy Btu/lb
H.P.	Horse power, measure of work done on the air
M	Mach number
M_c	Compressor Mach number, u/a_{01}
M_c'	Nominal M_c (Result of grouping and averaging)
N	Speed of compressor, r.p.m.
P	Total pressure, psia
R	Gas constant, 53.35 ft lbf/lbm ^o R for air
R_e	Reynolds number
R_e'	Nominal R_e (Result of grouping and averaging)
T	Total temperature, ^o R
a	Speed of sound, ft/sec
c	Mean chord of compressor blade, ft
g	Standard acceleration of gravity, 32.17 ft/sec ²
i	Indicated (Subscript)
k	Ratio of specific heats
p	Static pressure, psia
s	Stator; isentropic (Subscript)
t	Static temperature ^o R
u	Tip speed of compressor rotor blades ft/sec
v	Air velocity
w	Air flow, lbm/sec
α	Thermocouple recovery factor, $(T_1 - t)/(T - t)$
δ	Ratio of inlet total pressure to standard sea level pressure

- η Efficiency
- ρ Density, lbm/sec
- θ Ratio of inlet total temperature to standard sea level temperature
- μ Viscosity

Numerical Subscripts

- 0 Measuring station zero; total (stagnation) inlet value; normal (rated) value
- 0, 1, 1R, 1S, etc., 2, denote measuring stations

Calculations

Appendix (B)

The calculations in this thesis were simplified considerably by the information contained in Reference (d), by the availability of the air flow calibration data in Reference (c), and by the fact that relatively low velocities were encountered at the temperature measuring stations. It should be noted that the air flow calibration curve in Reference (c) is incorrectly plotted for general use. This was replotted using the ratio of the pressure difference across the nozzle to the inlet pressure as an ordinate. A procedure is outlined in Reference (d) for obtaining the outlet total pressure from the measured outlet static pressure, the air flow, the annulus area, and the indicated outlet temperature. The procedure involves use of the following basic equations which are derived in that report:

$$P_2 = p_2 (Y_2 + 1)^{k/k-1}$$

$$Y_2 = \frac{-1 + \sqrt{1 + \frac{2(k-1)R}{kg} \frac{\alpha w_{T12}^2}{p_2^2 A_2^2}}}{2\alpha}$$

These equations are plotted in Fig. (18) of the report as P_2/p_2 versus $w_{T12}^2/p_2^2 A_2^2$ with α as a parameter.

A curve of recovery factor, α , versus air velocity was also presented in Reference (d) for thermocouples similar to those used at the compressor outlet measuring station. Utilizing the indicated temperature, static pressure and

area at the outlet, a first estimate of the velocity was obtained in order to find the recovery factor. Then, with P_{02}/P_2 from Figure (18), the temperatures could have been obtained from the isentropic relations:

$$(A) \quad t_2 = \frac{T_{12}}{\left[\left(\frac{P_2}{P_1} \right)^{\frac{k-1}{k}} - 1 \right] \alpha + 1}$$

$$(B) \quad T_2 = t_2 (P_2/P_1)^{\frac{k-1}{k}}$$

As will be shown in the sample calculations to follow, considering the low air velocities attained, the error introduced by assuming $T_{12} = T_1$ did not warrant the added complication of the above calculation in most cases. Run No. 43 was chosen in the sample to illustrate a conservative estimate of the smallness of this error.

Sample Calculation

Entering the air flow curve with $(P_0 - P_1)/P_0$

find

$$(1) \quad 100 w \sqrt{T_1/P_0} = 12.52$$

Then

$$(2) \quad w = 12.52 \quad P_0(\text{in Hg})/100 \sqrt{T_1} = \frac{12.46 \times 7.52}{100 \times 23.45}$$

$$= 4.01 \text{ lbm/sec}$$

and, with $P_2(\text{in Hg})$ and $A_2(\text{in}^2)$

$$(3) \quad w^2 T_{12}/P_2^2 A_2^2 = \frac{(4.01)^2 (627)}{(19.76)^2 (19.6)^2} = 0.0671$$

Now

$$(4) \quad f_2 \cong p_2 / RT_{i2} = \frac{19.76 \times 144}{53.35 \times 627} = 0.085 \text{ lb/ft}^3$$

and

$$(5) \quad v_2 = w / f_2 A_2 \cong \frac{4.0 \times 144}{0.085 \times 19.6} = 346 \text{ ft/sec}$$

From Figure 7, Reference (d)

$$(6) \quad \alpha = 0.92$$

From Figure 18, Reference (d), entering with (3)

$$(7) \quad p_2 / p_2 = 1.06$$

Using equations (A) and (B)

$$(8) \quad t_2 = 627 / [(1.06)^{.286} - 1] 0.92 + 1$$

$$= 627 / 1.0146 = 618.5^\circ\text{R}$$

$$(9) \quad T_2 = 618.5 (1.06)^{.286} = 627.8^\circ\text{R}$$

$$\text{Then } T_2 - T_{i2} = 0.8^\circ\text{R}$$

Assuming $T_2 = T_{i2}$ would introduce an error of only 0.127 % in T_2 or an error of 1.03 % in $(T_2 - T_1)$. For a majority of cases the error was far smaller and was neglected.

From the Gas Tables

$$H_1 = 131.34 \text{ Btu/lb}$$

$$H_2 = 149.96 \text{ Btu/lb}$$

$$H_{2s} = 145.9 \text{ Btu/lb}$$

Then

$$H_2 - H_1 = 18.62$$

$$H_{2s} - H_1 = 14.56$$

and

$$(10) \quad \text{HP} = w(H_2 - H_1)778/550 = 4.0 \times 14.56 \times 778/550$$

$$= 82.4 \text{ HP}$$

also

$$(11) \quad \gamma_c = (H_{2s} - H_1)/(H_2 - H_1) = 0.782$$

Now

$$(12) \quad u = 2\pi rR/60 \times 12 = 2\pi (3.93) \times 20,050/60 \times 12 \\ = 755 \text{ ft/sec}$$

and

$$(13) \quad a_{01} = 49.1 \sqrt{T_1} = 1151 \text{ ft/sec}$$

Then

$$(14) \quad M_c = u/a_{01} = 755/1151 = 0.655$$

Also

$$(15) \quad \rho_{01} = P_1/RT_1 = 14.53 \times 144/53.35 \times 549.5 \\ = 0.0714 \text{ lbm/ft}^3$$

and from the Gas Tables

$$(16) \quad \mu_{01} = 126.4 \text{ lbm/sec ft}$$

Then, using the chord of the first set of rotor blades as the characteristic length

$$(17) \quad R_e = \rho_{01} u c_1 / \mu_{01} = .0714 \times 755 \times 0.864/126.4 \times 12 \\ = 307,000$$

Finally, since

$$\delta = P_{01}/P_{s1} = 0.99, \text{ and} \quad \sqrt{\theta} = \sqrt{T_{01}/T_{s1}} \\ = 1.03$$

$$\text{Then } w \sqrt{\theta} / \delta = 4 \times 1.03 / .99 = 4.16 \text{ lbm/sec}$$

$$\text{and } w \sqrt{\theta} / w_o \delta = 4.16 / 6.8 = 0.612$$

References

- a) Wallner, Lewis E., and Fleming, William A., "Reynolds Number Effect on Axial Flow Compressor Performance", NACA RM E9G11, September 15, 1949.
- b) Handbook of Service Instructions with Parts Catalog for Turbo Jet Engines Model XJ32-W^E-4 (X9.5B), Bureau of Aeronautics, NavAer 02B-110-502, May 1, 1948.
- c) Swainson, Gustav F., Jr., Padis, Alexander A., and Gern, Charles A., "A Compressor Test Facility", Masters Thesis, Mass. Inst. of Tech., 1951.
- d) NACA Subcommittee on Compressors, "Standard Procedures for Rating and Testing Multistage Axial Flow Compressors", NACA TN 1138, September 1946.
- e) Baker, Dean H., "Manual on Thermometry", Pratt and Whitney Division, United Aircraft Corporation, East Hartford, Connecticut, 1950.

Bibliography

1. Hottel, H. C., and Katinsky A., "Temperature Measurements in High Velocity Air Streams", Journal of Applied Mechanics, Vol. 12, No. 1, March 1945, pp A-25 to A-32.
2. Boyle, Roy E., "An Investigation of the Influence of Orifice Geometry on Static Pressure Measurements", Masters Thesis, Mass. Inst. of Tech., June 1949.
3. ASME Power Test Codes; Pressure Measurement, Part 2, Chapter 2; Temperature Measurement, Part 3, Chapter 3.

TABLE I
COMPRESSOR PERFORMANCE DATA

Run Number	Compressor Mach Number	Nominal Compressor Mach Number	Reynolds Number	Nominal Reynolds Number	Inlet Total Pressure (psia)	Outlet Total Pressure (psia)	Total Pressure Ratio	Inlet Total Temperature (or)	Outlet Total Temperature (or)	Inlet Stagnation Density (lb/ft ³)	Air Flow (lb/sec)	Corrected Air Flow (lb/sec)	Corrected Fraction of Rated Air Flow	R.P.M.	Efficiency	Compressor Horse Power
	M_c	M_c^1	R_e	R_e^1	P_1	P_2	P_2/P_1	T_1	T_2	ρ_{01}	W	$\frac{W\sqrt{\theta}}{\delta}$	$\frac{W\sqrt{\theta}}{\delta W_0}$	N	η_c	HP
1	0.431	0.431	232,500	232,500	11.29	14.73	1.306	527.8	586.8	0.0576	2.94	3.87	0.570	20,050	70.5	59.1
2	0.463	0.461	115,100	115,100	7.18	8.36	1.165	516.9	549.3	0.0374	1.36	2.78	0.394	15,100	71.0	14.97
3	0.464	0.461	126,000	126,000	7.84	10.50	1.340	515.8	577.4	0.0409	0.96	1.79	0.263	15,100	72.6	20.1
4	0.462	0.461	162,800	162,800	10.22	13.39	1.310	520.4	574.8	0.0530	1.39	2.00	0.294	15,100	76.0	25.8
5	0.454	0.461	172,900	175,100	10.97	12.72	1.160	520.9	551.5	0.0569	2.12	2.85	0.419	15,000	73.0	22.1
6	0.467	0.461	176,000	175,100	11.15	12.97	1.163	520.3	552.3	0.0579	2.19	2.90	0.426	15,050	71.4	24.0
7	0.455	0.461	176,500	175,100	11.14	13.02	1.170	520.7	553.4	0.0579	2.14	2.82	0.415	15,050	72.6	23.8
8	0.485	0.489	114,900	114,900	6.86	8.25	1.202	521.1	556.2	0.0355	1.38	2.98	0.439	15,930	78.4	16.8
9	0.490	0.489	146,900	146,900	8.71	10.67	1.224	522.8	562.3	0.0450	1.74	2.96	0.435	16,100	74.1	23.8
10	0.490	0.489	170,000	170,000	10.09	13.71	1.360	523.5	590.6	0.0520	1.42	2.09	0.308	16,150	71.7	32.4
11	0.491	0.489	193,800	193,800	11.65	13.64	1.171	526.3	562.0	0.0596	2.40	3.06	0.450	16,150	68.2	29.2
12	0.551	0.546	127,700	137,400	6.74	9.86	1.464	522.9	606.7	0.0348	1.12	2.45	0.360	18,100	71.6	31.7
13	0.550	0.546	133,000	137,400	7.08	9.75	1.380	525.4	589.3	0.0364	1.47	3.06	0.450	18,100	79.2	31.8
14	0.546	0.546	143,500	137,400	7.70	9.43	1.225	526.4	572.8	0.0395	1.26	2.43	0.357	17,950	67.6	19.8
15	0.547	0.546	144,900	137,400	7.75	9.40	1.213	524.8	571.1	0.0399	1.81	3.46	0.519	18,000	62.9	29.0
16	0.550	0.546	178,500	178,500	9.47	13.73	1.450	523.9	561.6	0.0489	1.46	2.27	0.334	18,050	63.5	45.7
17	0.548	0.546	189,200	189,200	10.18	13.63	1.340	526.0	585.3	0.0521	2.20	3.20	0.470	18,050	77.3	44.2
18	0.547	0.546	209,500	209,500	11.30	14.07	1.245	526.3	572.0	0.0579	2.67	3.50	0.515	18,000	74.6	41.5
19	0.541	0.546	262,000	263,100	14.63	20.70	1.414	538.5	610.7	0.0735	2.78	2.84	0.418	18,000	77.5	68.0
20	0.541	0.546	262,500	263,100	14.61	19.87	1.360	537.5	599.1	0.0735	3.10	3.18	0.468	18,000	79.4	64.9
21	0.546	0.546	264,000	263,100	14.65	21.35	1.459	537.9	625.5	0.0735	2.11	2.16	0.318	18,150	69.7	62.6
22	0.543	0.546	264,000	263,100	14.60	18.08	1.238	533.8	580.1	0.0738	3.45	3.52	0.517	17,950	72.7	54.1
23	0.565	0.565	216,500	216,500	11.25	14.30	1.271	525.1	574.3	0.0579	2.76	2.96	0.531	18,600	77.9	46.2
24	0.608	0.605	135,300	136,400	6.59	9.74	1.479	529.1	609.2	0.0336	1.54	3.48	0.511	20,050	78.2	41.9
25	0.606	0.605	137,500	136,400	6.40	10.10	1.579	520.6	625.1	0.0338	1.22	2.83	0.416	20,050	69.4	43.4

TABLE I (Continued)
COMPRESSOR PERFORMANCE DATA

Run Number	Compressor Mach Number	Nominal Compressor Mach Number	Reynolds Number	Nominal Reynolds Number	Inlet Total Pressure (psia)	Outlet Total Pressure (psia)	Total Pressure Ratio	Inlet Total Temperature (or)	Outlet Total Temperature (or)	Inlet Stagnation Density (lb/ft ³)	Air Flow (lb/sec)	Corrected Air Flow (lb/sec)	Corrected Fraction of Rated Air Flow	R.P.M.	Efficiency	Compressor Horse Power
	M_c	M_c^1	R_e	R_e^1	P_1	P_2	P_2/P_1	T_1	T_2	ρ_{01}	W	$\frac{W\sqrt{\theta}}{\delta}$	$\frac{W\sqrt{\theta}}{\delta W_0}$	N	η_c	HP
26	0.610	0.605	155,500	155,500	7.43	9.83	1.323	523.7	583.2	0.0383	1.93	3.84	0.565	20,050	73.3	39.2
27	0.610	0.605	186,500	186,500	9.02	14.51	1.609	526.9	630.5	0.0461	1.78	2.93	0.431	20,100	73.9	62.7
28	0.606	0.605	193,800	196,300	9.56	14.61	1.528	534.5	622.4	0.0484	2.08	3.25	0.478	20,050	77.9	62.1
29	0.605	0.605	198,800	196,300	9.81	12.75	1.300	534.0	593.2	0.0496	2.54	3.87	0.570	20,050	70.0	51.1
30	0.609	0.605	219,500	219,500	10.62	14.23	1.340	529.0	590.9	0.0544	2.74	3.82	0.561	20,100	74.2	57.7
31	0.599	0.605	285,000	287,400	14.60	22.10	1.513	544.7	636.4	0.0724	3.09	3.19	0.469	20,050	74.4	96.3
32	0.600	0.605	285,500	287,400	14.57	20.10	1.380	543.0	610.3	0.0724	3.56	3.69	0.543	20,050	77.6	81.4
33	0.601	0.605	289,000	287,400	14.63	22.90	1.564	542.1	653.6	0.0729	2.56	2.63	0.387	20,100	66.1	97.0
34	0.605	0.605	290,000	287,400	14.56	18.88	1.298	539.1	595.9	0.0729	3.82	3.94	0.579	20,100	73.6	73.6
35	0.664	0.658	189,200	194,000	8.47	13.24	1.564	532.7	604.8	0.0429	2.24	3.94	0.580	22,000	97.3	54.7
36	0.660	0.658	198,800	194,000	8.86	15.25	1.720	528.4	644.7	0.0454	2.09	3.48	0.511	21,800	76.1	82.7
37	0.659	0.658	210,500	212,600	9.73	16.03	1.648	541.4	652.8	0.0485	1.91	2.95	0.434	22,000	74.2	72.3
38	0.660	0.658	213,000	212,600	9.81	14.52	1.480	539.8	623.5	0.0496	2.34	3.57	0.525	21,950	76.4	66.5
39	0.658	0.658	213,500	212,600	9.79	13.16	1.343	536.9	605.5	0.0492	2.46	3.75	0.551	21,900	68.5	57.1
40	0.660	0.658	213,500	212,600	9.82	16.65	1.696	540.8	661.0	0.0490	1.77	2.71	0.398	22,050	73.0	72.3
41	0.654	0.658	304,000	307,300	14.54	22.75	1.564	552.1	645.9	0.0711	3.77	3.94	0.580	22,050	80.0	120.1
42	0.654	0.658	306,000	307,300	14.57	24.7	1.695	551.1	667.0	0.0714	3.48	3.63	0.534	22,000	77.0	143.0
43	0.655	0.658	307,000	307,300	14.53	20.9	1.440	549.5	627.0	0.0714	4.01	4.16	0.612	22,050	78.2	105.2
44	0.655	0.658	312,000	307,300	14.54	19.58	1.346	545.5	613.1	0.0720	4.15	4.30	0.632	21,950	71.0	95.5
45	0.683	0.680	177,000	177,000	7.64	13.63	1.785	527.0	660.1	0.0391	1.73	3.35	0.492	22,550	71.1	78.4
46	0.681	0.680	244,000	247,000	10.56	14.76	1.399	529.3	602.2	0.0540	3.17	4.46	0.656	22,500	72.4	79.2
47	0.676	0.680	250,500	247,000	10.98	15.30	1.394	528.7	601.3	0.0560	3.30	4.60	0.676	22,300	71.6	82.0
48	0.709	0.709	217,500	217,500	9.04	13.09	1.449	528.4	608.9	0.0462	2.82	4.64	0.681	23,400	72.7	77.7
49	0.751	0.751	146,000	146,000	5.85	8.45	1.445	535.6	626.0	0.0295	1.13	2.88	0.424	25,000	65.8	34.7
50	0.765	0.765	184,200	184,200	7.32	10.80	1.476	540.6	634.5	0.0366	1.93	3.96	0.582	25,550	67.7	61.5

TABLE II
SURVEY OF STATIC PRESSURES

Run	P ₁	P _{1R}	P _{1S}	P _{2R}	P _{2S}	P _{3R}	P _{3S}	P _{4R}	P _{4S}	P _{5R}	P _{5S}	P _{6R}	P _{6S1}	P _{6S2}	P ₂
1	10.91	10.92	11.44	11.84	12.14	12.56	13.00	13.18	13.40	13.59	13.39	13.00	12.19	13.22	13.90
2	7.06	7.06	7.28	7.44	7.53	7.67	7.83	7.92	7.98	7.01	7.94	7.81	7.72	7.87	8.06
3	7.79	7.88	8.01	8.19	8.31	8.51	8.69	8.93	9.21	9.35	9.54	9.7	9.93	10.03	10.12
4	10.13	10.19	10.47	10.67	10.90	11.16	11.46	11.66	12.01	12.20	12.46	12.61	12.84	13.05	13.16
5	10.77	10.80	11.11	11.31	11.40	11.67	11.90	11.00	12.10	12.17	12.02	11.80	11.65	11.90	12.24
6	10.94	10.97	11.28	11.50	11.65	11.87	12.12	12.22	12.30	12.39	12.24	12.02	11.85	12.12	12.46
7	10.94	10.97	11.29	11.51	11.63	11.88	12.12	12.23	12.32	12.40	12.28	12.10	10.95	12.20	12.54
8	6.74	6.86	6.98	7.16	7.25	7.42	7.60	7.70	7.78	7.83	7.76	7.63	7.51	7.68	7.92
9	8.54	8.55	8.86	9.05	9.20	9.40	9.66	9.78	9.99	10.01	9.94	9.84	9.74	9.76	10.26
10	9.99	10.08	10.33	10.57	10.79	11.09	11.41	11.69	12.12	12.30	12.68	12.91	13.20	13.35	13.52
11	11.24	11.28	11.63	11.89	12.16	12.30	12.60	12.72	12.73	12.93	12.76	12.51	12.29	12.62	13.05
12	6.65	6.74	6.93	7.15	7.32	7.57	7.83	8.06	8.42	8.59	8.90	9.10	9.35	9.51	9.63
13	6.93	6.95	7.27	7.50	7.65	7.89	8.16	8.34	8.58	8.70	8.85	8.90	8.96	9.17	9.42
14	7.60	7.47	7.73	7.96	8.09	8.31	8.56	8.69	8.80	8.89	8.93	8.56	8.38	8.61	9.19
15	7.54	7.56	7.84	8.09	8.21	8.44	8.70	8.82	8.95	9.01	8.92	8.73	8.55	8.81	9.15
16	9.36	9.55	9.75	10.08	10.29	10.67	10.96	11.30	11.75	12.04	12.42	12.75	13.10	13.27	13.47
17	9.95	9.99	10.44	10.74	10.96	11.28	11.67	11.85	12.15	12.34	12.39	12.38	12.44	12.74	13.11
18	10.99	11.06	11.46	11.79	12.02	12.32	12.70	12.86	13.07	13.13	12.98	12.65	12.42	12.86	13.37
19	14.36	14.45	15.14	15.59	16.02	16.47	17.03	17.40	18.06	18.31	18.75	19.00	19.41	19.76	20.11
20	14.27	14.33	15.00	15.44	15.77	16.22	16.78	17.06	17.58	17.75	17.98	18.02	18.20	18.65	19.12
21	14.45	14.64	15.06	15.49	15.93	16.47	17.03	17.52	18.32	18.72	19.36	20.31	20.47	20.74	20.99
22	14.18	14.26	14.78	15.17	15.49	15.85	16.35	16.52	16.84	16.86	16.64	16.17	15.93	16.47	17.13
23	10.92	10.99	11.41	11.78	12.15	12.36	12.76	12.95	12.76	13.11	13.30	13.13	12.81	12.52	13.55
24	6.41	6.39	6.82	7.06	6.24	7.50	7.82	7.99	8.35	8.46	8.66	8.75	8.88	9.08	9.36
25	6.28	6.38	6.64	6.89	7.15	7.38	7.68	7.92	8.36	8.59	8.95	9.25	9.62	9.74	9.83

TABLE II (Continued)
SURVEY OF STATIC PRESSURES

Run	P ₁	P _{1R}	P _{1S}	P _{2R}	P _{2S}	P _{3R}	P _{3S}	P _{4R}	P _{4S}	P _{5R}	P _{5S}	P _{6R}	P _{6S1}	P _{6S2}	P ₇
26	7.19	7.19	7.53	7.81	7.91	8.25	8.57	8.71	8.95	9.12	8.94	8.72	8.51	8.85	9.30
27	8.95	9.05	9.50	9.82	10.18	10.65	11.14	11.45	12.19	12.36	12.98	13.26	13.77	13.96	14.17
28	9.34	9.35	10.00	10.35	10.64	11.03	11.50	11.80	12.34	12.56	12.90	13.08	14.42	13.82	14.14
29	9.47	9.49	9.91	10.25	10.47	10.79	11.21	11.37	11.59	11.75	11.55	11.24	10.95	11.40	11.95
30	10.26	10.27	10.77	11.14	11.41	11.76	12.24	12.44	12.77	12.91	12.82	12.59	12.44	12.91	13.48
31	14.26	14.31	15.19	15.71	16.21	16.80	17.50	17.92	18.75	19.09	19.84	19.92	20.50	20.92	21.37
32	14.12	14.13	14.88	15.40	15.78	16.30	16.95	17.20	17.77	17.94	18.42	17.89	17.94	18.53	19.20
33	14.41	14.64	15.17	15.68	16.20	16.89	17.52	18.10	19.02	19.56	20.40	20.94	21.70	22.06	22.36
34	14.04	14.06	14.72	15.24	15.59	16.08	16.67	16.91	17.28	17.37	17.12	16.57	16.14	16.86	17.72
35	8.18	8.16	8.72	9.10	9.39	9.80	10.31	10.60	11.10	11.31	11.56	11.64	11.78	12.24	12.69
36	8.62	8.86	8.72	8.64	9.32	9.72	10.16	10.60	10.16	11.59	12.27	12.59	13.55	14.46	14.75
37	9.38	9.34	10.02	10.48	10.92	11.41	11.95	12.46	13.18	13.47	14.16	14.41	14.99	15.28	15.63
38	9.54	9.44	9.99	10.40	10.72	11.2.	11.75	12.1	12.54	12.66	13.08	12.68	12.73	13.25	13.96
39	9.48	9.35	9.84	10.28	10.56	10.92	11.46	11.68	12.00	12.12	12.42	11.58	11.23	11.80	12.49
40	9.66	9.63	10.29	10.77	11.21	11.75	12.34	13.91	13.59	13.96	14.7	115.02	15.68	15.98	16.30
41	14.02	13.96	14.99	15.61	16.09	16.80	17.65	18.09	18.97	19.27	20.07	19.91	20.40	21.09	21.73
42	14.18	14.20	15.27	15.92	16.80	17.31	18.20	18.82	19.96	20.45	21.58	21.92	22.87	23.40	23.86
43	13.94	13.92	14.75	15.36	15.83	16.47	17.22	17.55	18.23	18.37	18.98	18.14	18.12	18.90	19.76
44	13.91	13.88	14.64	15.24	15.86	16.24	16.95	17.23	17.72	17.80	18.26	16.89	16.34	17.24	18.24
45	7.45	7.44	8.04	8.45	8.77	9.21	9.80	10.20	10.88	11.22	11.89	12.32	12.87	13.09	13.29
46	10.08	10.27	10.62	11.11	11.42	11.90	12.58	12.75	13.08	13.38	13.19	12.71	12.24	12.95	13.77
47	10.48	10.49	11.05	11.56	11.88	12.39	12.98	13.25	13.50	13.79	13.59	13.18	12.71	13.42	14.27
48	8.58	8.55	9.05	9.51	9.79	10.24	10.78	11.05	11.29	11.56	11.42	11.10	11.68	11.45	12.17
49	5.85	5.49	5.86	6.20	6.42	6.79	7.18	7.38	7.68	7.85	8.12	7.60	7.34	7.82	8.21
50	7.05	6.79	7.20	7.68	7.97	8.41	8.95	9.19	9.45	9.74	10.09	9.37	9.05	9.79	10.28

Note: All pressures in pounds per square inch absolute.

TABLE III
SUMMARY OF DIMENSIONLESS PERFORMANCE VARIABLES

Run	M_c^{-1}	R_e^{-1}	η_c	P_2/P_1	$\frac{W\sqrt{\theta}}{\delta W_0}$
1	0.431	232,500	70.5	1.306	0.570
2	0.461	115,100	71.0	1.165	0.394
3	0.461	126,000	72.6	1.340	0.263
4	0.461	162,800	76.0	1.310	0.294
5	0.461	175,100	73.0	1.160	0.419
6	0.461	175,100	71.4	1.163	0.426
7	0.461	175,100	72.6	1.170	0.415
8	0.489	114,900	78.4	1.202	0.439
9	0.489	146,900	74.1	1.224	0.435
10	0.489	170,000	71.7	1.360	0.308
11	0.489	193,800	68.2	1.171	0.450
12	0.546	137,400	71.6	1.464	0.360
13	0.546	137,400	79.2	1.380	0.450
14	0.546	137,400	67.6	1.225	0.357
15	0.546	137,400	62.9	1.213	0.519
16	0.546	178,500	63.5	1.450	0.334
17	0.546	189,200	77.3	1.340	0.470
18	0.546	209,500	74.6	1.245	0.515
19	0.546	263,100	77.5	1.414	0.418
20	0.546	263,100	79.4	1.360	0.468
21	0.546	263,100	69.7	1.459	0.318
22	0.546	263,100	72.7	1.238	0.517
23	0.565	216,500	77.9	1.271	0.531
24	0.605	136,400	78.2	1.479	0.511
25	0.605	136,400	69.4	1.579	0.416

TABLE III (Continued)
SUMMARY OF DIMENSIONLESS PERFORMANCE VARIABLES

Run	M_c'	Re'	ζ_c	P_2/P_1	$\frac{W \sqrt{\theta}}{\delta W_0}$
26	0.605	155,500	73.3	1.323	0.565
27	0.605	192,700	73.9	1.609	0.431
28	0.605	192,700	77.9	1.528	0.478
29	0.605	192,700	70.0	1.300	0.570
30	0.605	219,500	74.2	1.340	0.561
31	0.605	287,400	74.4	1.513	0.469
32	0.605	287,400	77.6	1.380	0.543
33	0.605	287,400	66.1	1.564	0.387
34	0.605	287,400	73.6	1.298	0.579
35	0.658	194,000	97.3	1.564	0.580
36	0.658	194,000	76.1	1.720	0.511
37	0.658	212,600	74.2	1.648	0.434
38	0.658	212,600	76.4	1.480	0.525
39	0.658	212,600	68.5	1.343	0.551
40	0.658	212,600	73.0	1.696	0.398
41	0.658	307,300	80.0	1.564	0.580
42	0.658	307,300	77.0	1.695	0.534
43	0.658	307,300	78.2	1.440	0.612
44	0.658	307,300	71.0	1.346	0.632
45	0.680	177,000	71.1	1.785	0.492
46	0.680	247,000	72.4	1.399	0.656
47	0.680	247,000	71.6	1.394	0.676
48	0.709	217,500	72.7	1.449	0.681
49	0.751	146,000	65.8	1.445	0.424
50	0.765	184,200	67.7	1.476	0.582

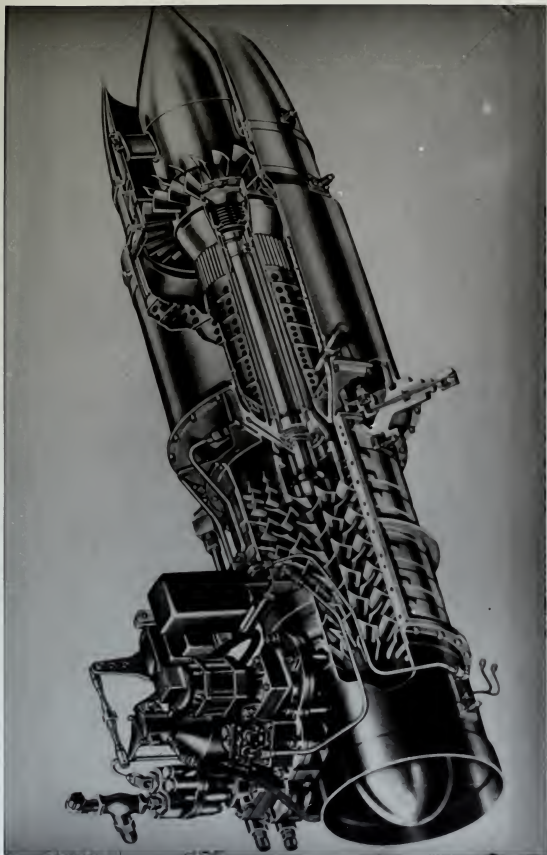


FIGURE 1
CUTAWAY VIEW OF WESTINGHOUSE X9.5B TURBO JET ENGINE

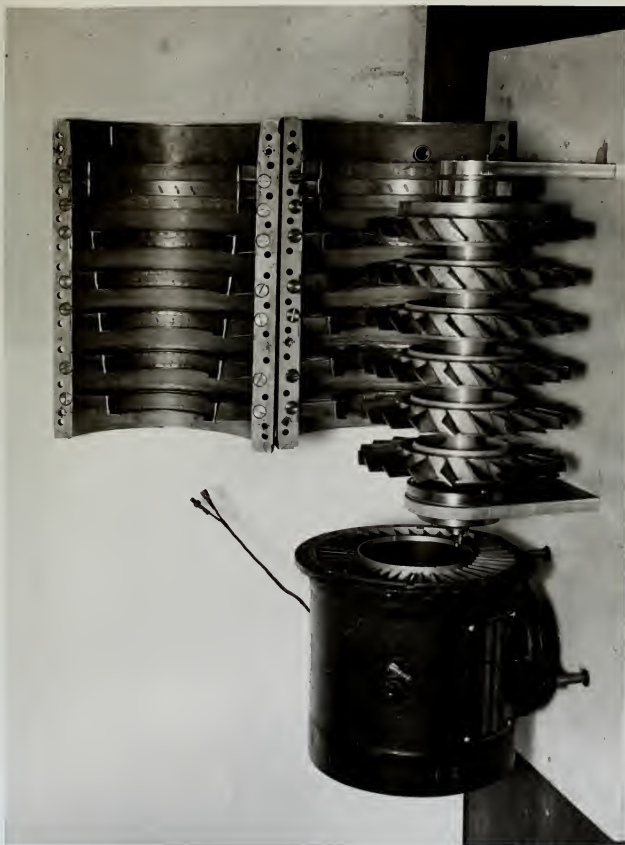


FIGURE 2
EXPLODED VIEW OF TEST COMPRESSOR

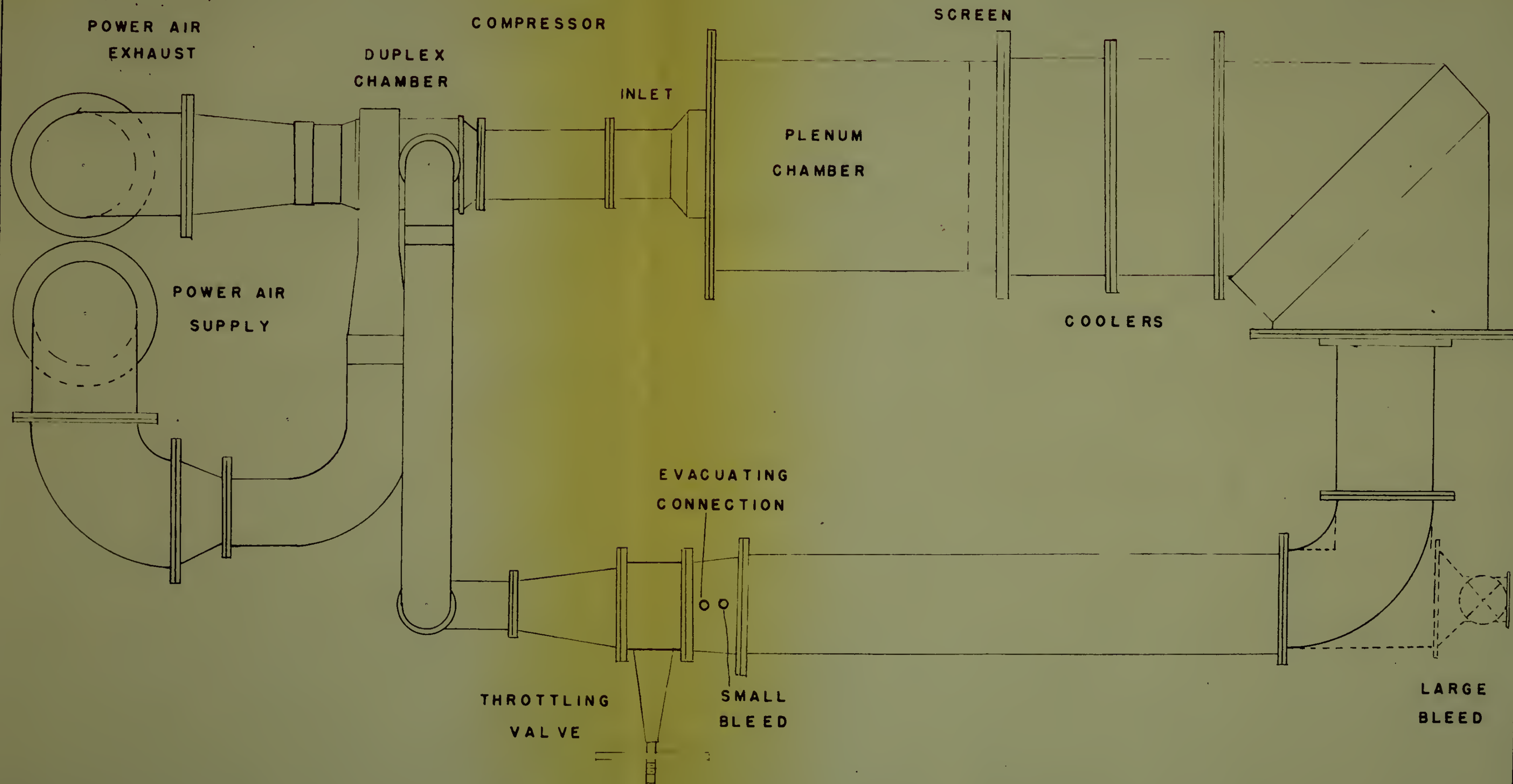


FIGURE 3
ARRANGEMENT OF COMPRESSOR TEST STAND

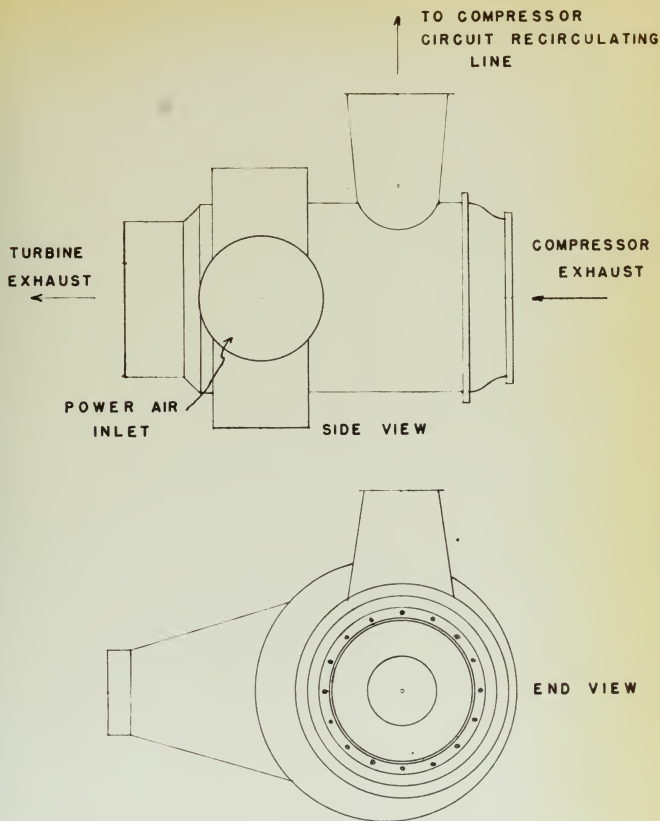


FIGURE 4

DUPLEX CHAMBER

SCHEMATIC VIEW OF EXTERNAL ARRANGEMENT

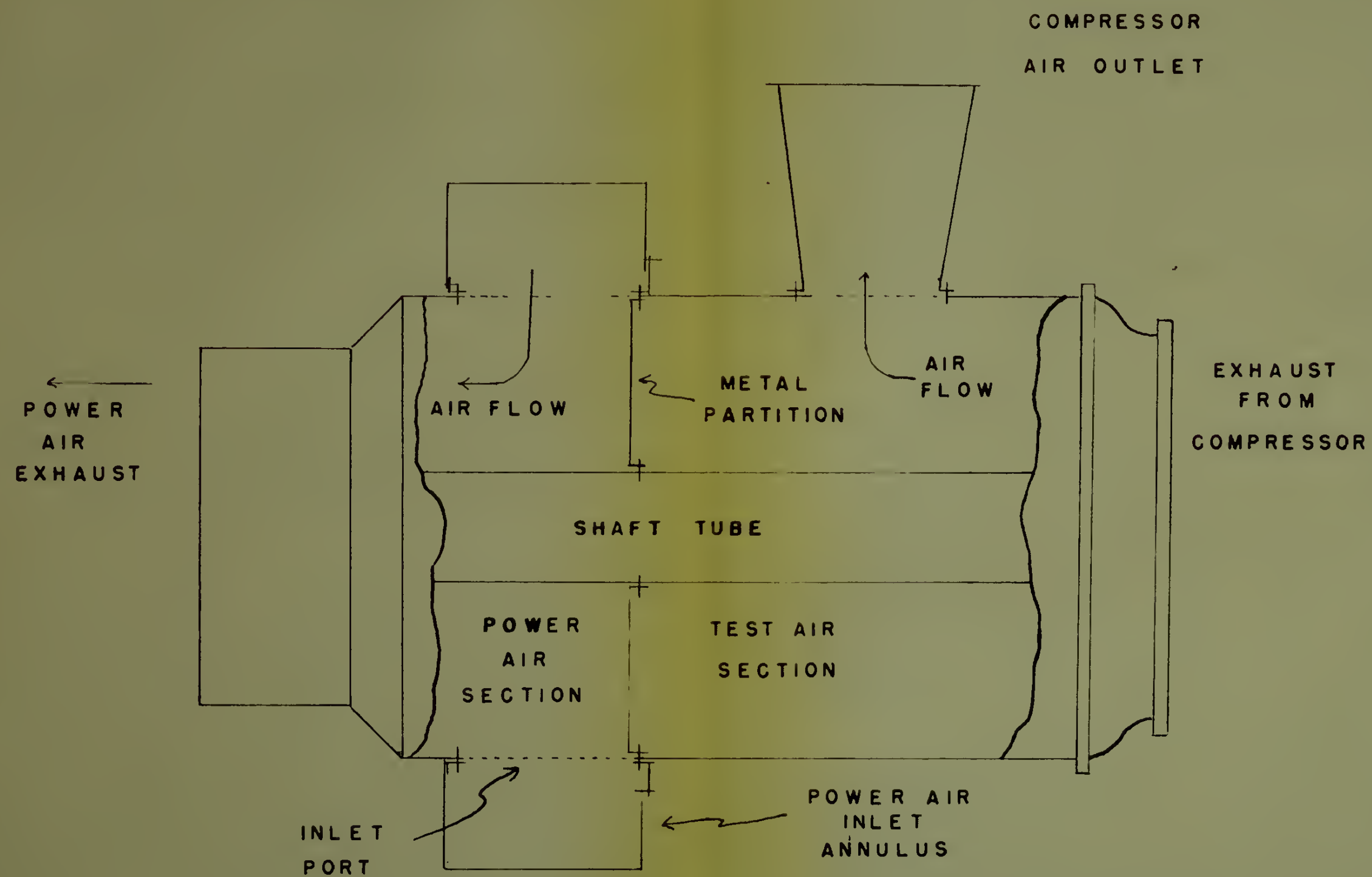
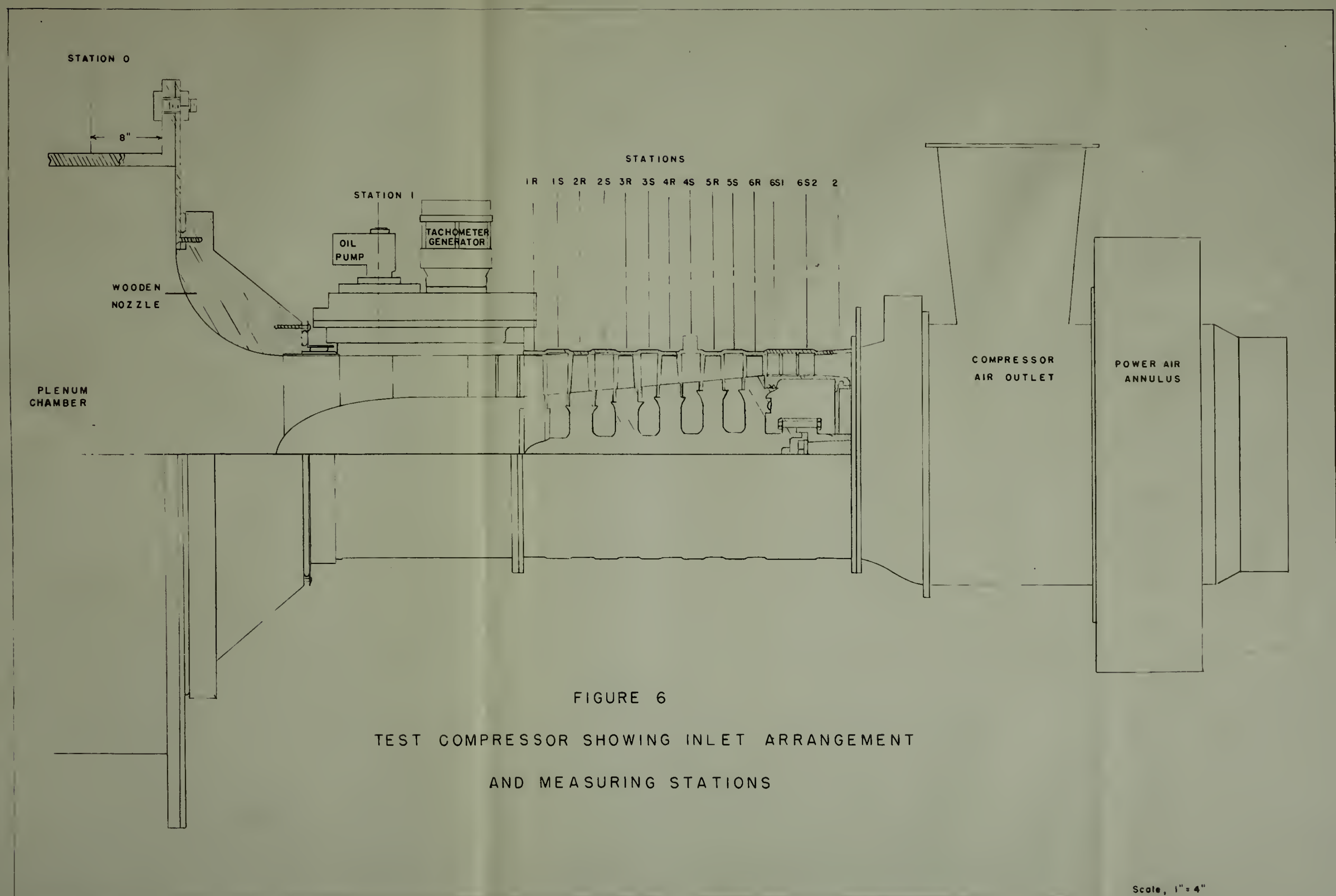
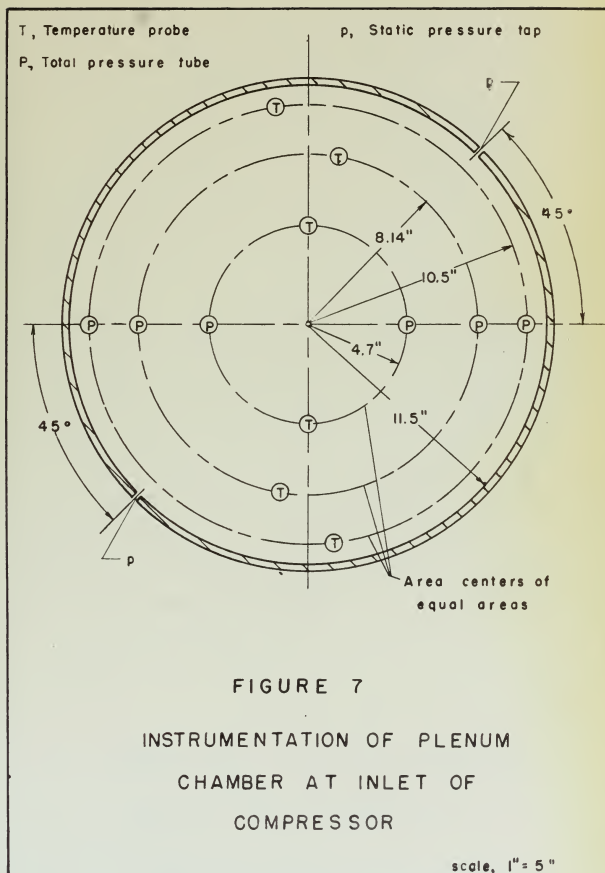


FIGURE 5

DUPLEX CHAMBER

SCHEMATIC VIEW OF INTERNAL ARRANGEMENT





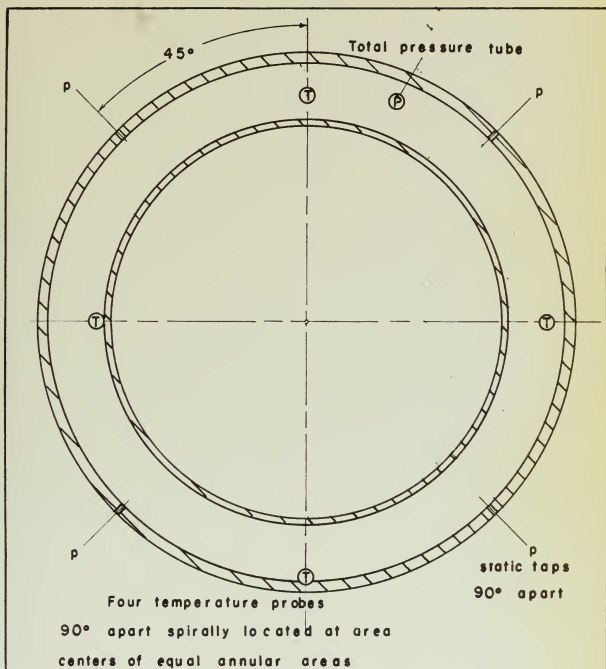


FIGURE 8

INSTRUMENTATION OF ANNULAR
OUTLET OF COMPRESSOR

scale, 1" = 1.6"

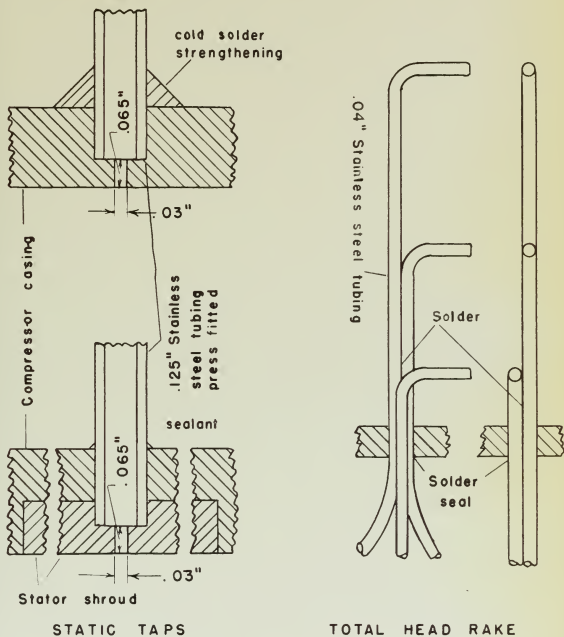


FIGURE 9
DETAILS OF PRESSURE
INSTRUMENTATION

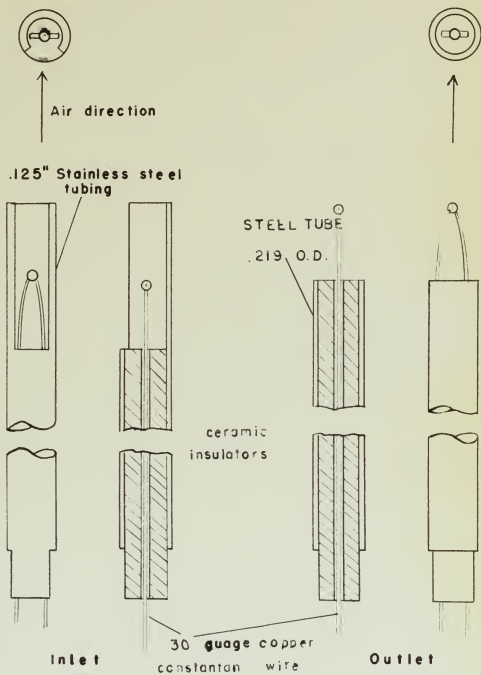


FIGURE 10
 DETAILS OF THE
 THERMOCOUPLE CONSTRUCTION

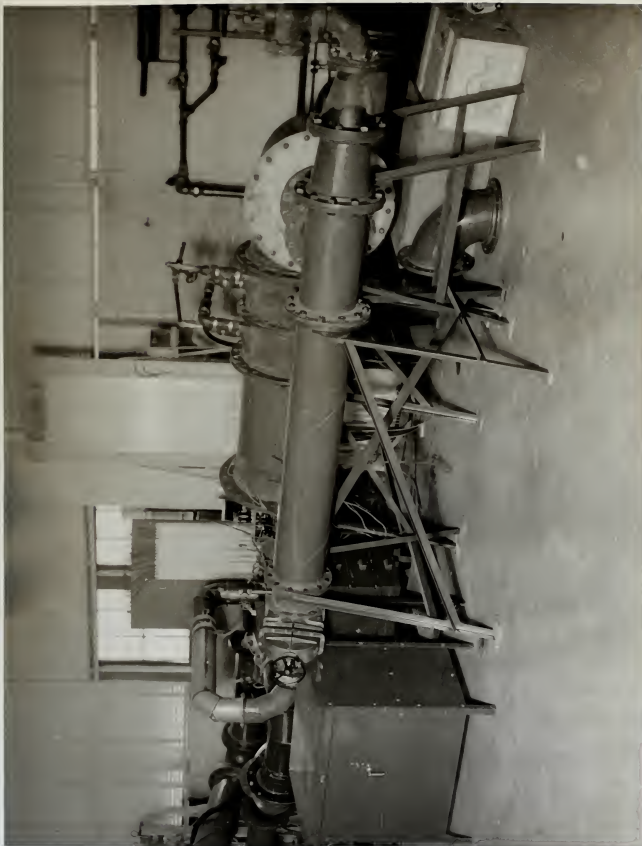
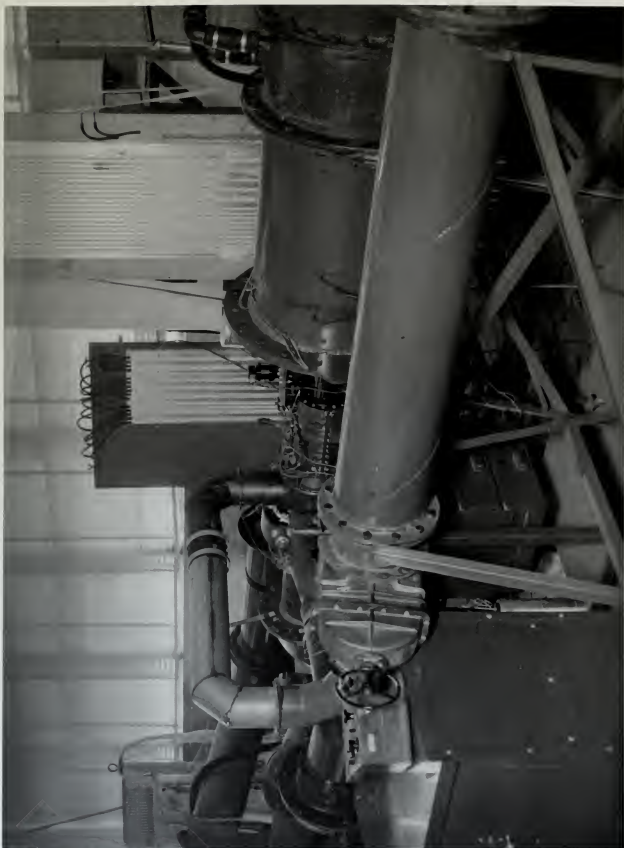


FIGURE 11
OVER-ALL VIEW OF COMPRESSOR TEST SET UP

FIGURE 12
INTERMEDIATE VIEW OF COMPRESSOR TEST SET UP



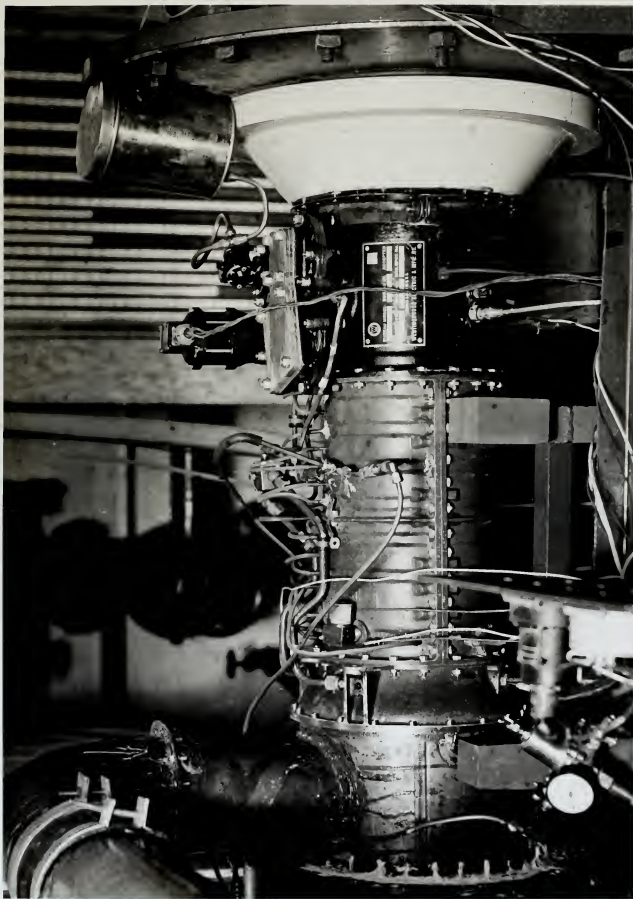


FIGURE 13
CLOSE-UP VIEW OF TEST COMPRESSOR

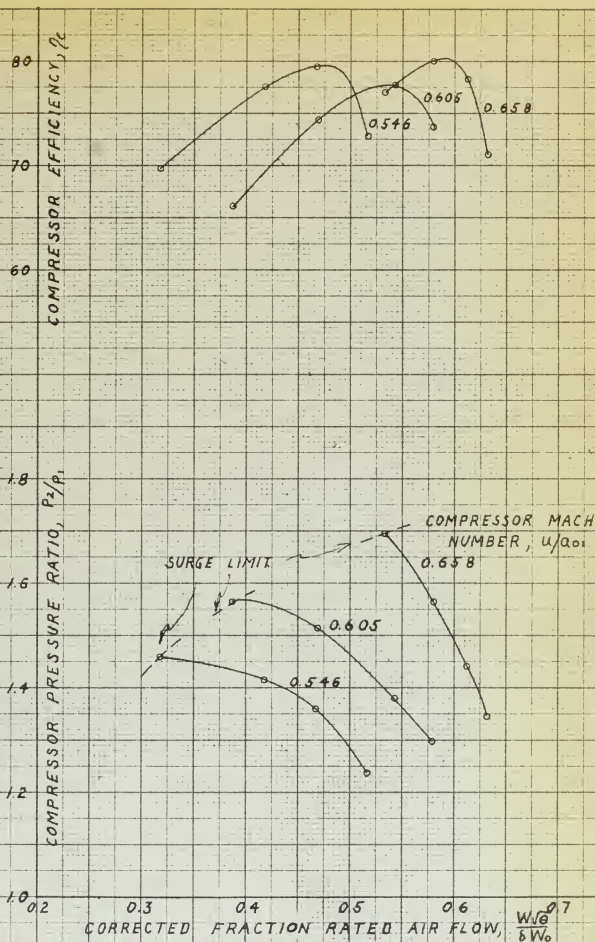


FIG. 14(a)
COMPRESSOR PERFORMANCE MAP

AVERAGE INLET DENSITY = 0.0726 lbs./cu. ft.

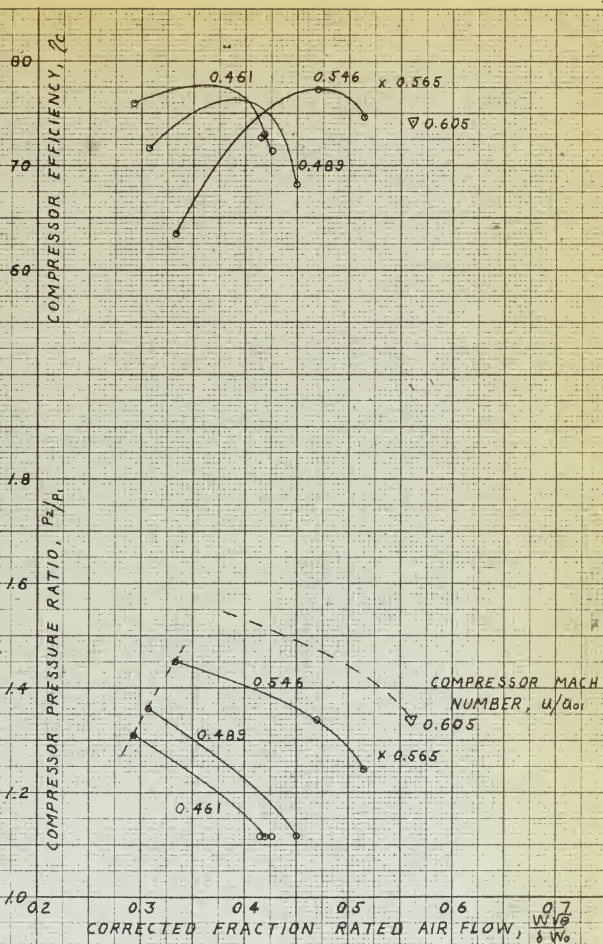


FIG. 14 (b)
 COMPRESSOR PERFORMANCE MAP
 AVERAGE INLET DENSITY = 0.0557 lbs./cu. ft.

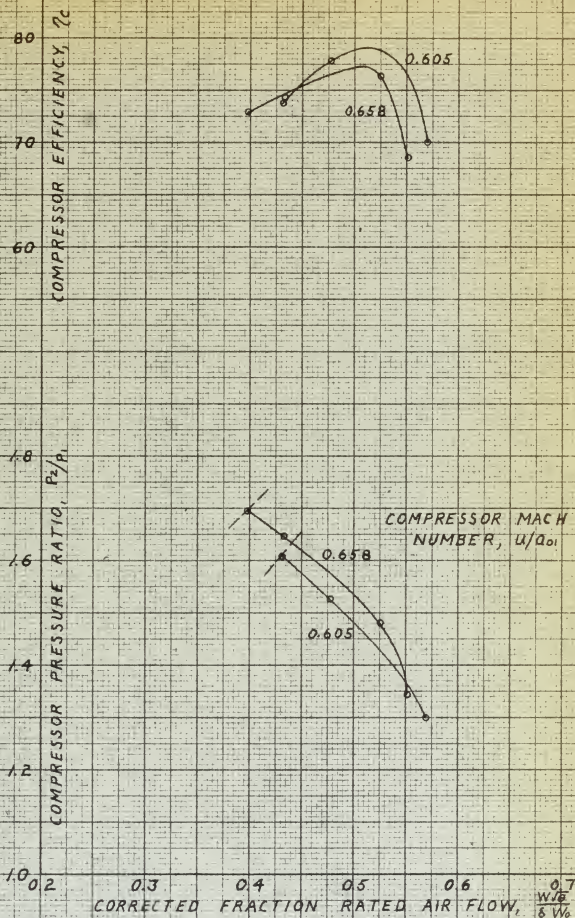


FIG. 14(c)
 COMPRESSOR PERFORMANCE MAP
 AVERAGE INLET DENSITY = 0.0485 lbs./cu. ft.

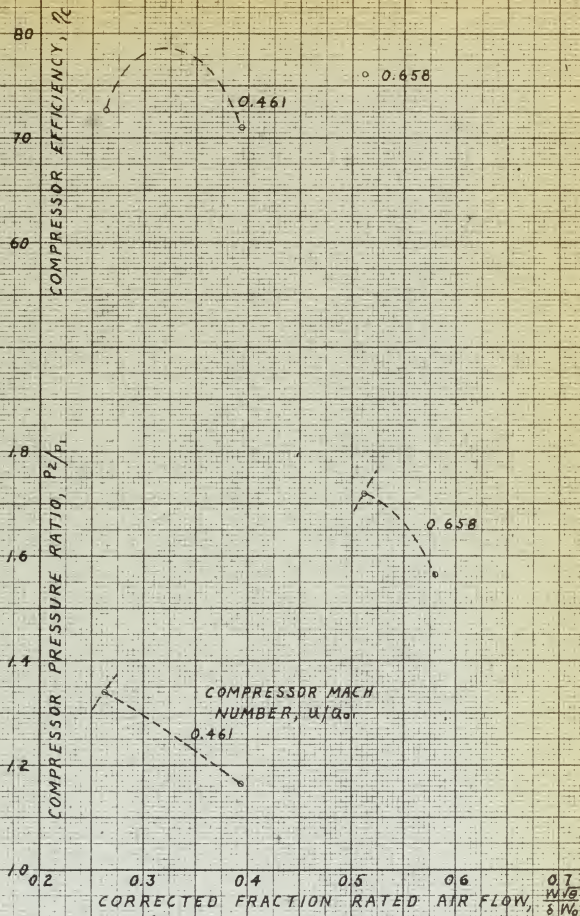


FIG. 14 (d)
 COMPRESSOR PERFORMANCE MAP
 AVERAGE INLET DENSITY = 0.0417 lbs./cu. ft.

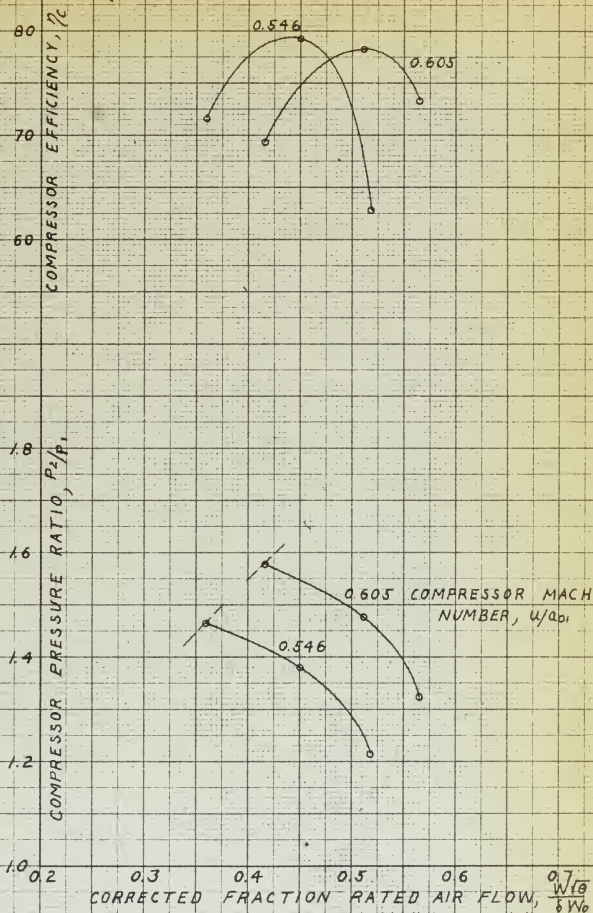


FIG. 14 (c)
COMPRESSOR PERFORMANCE MAP

AVERAGE INLET DENSITY = 0.0369 lbs/cu. ft.



FIGURE 15
MANOMETER BOARD SHOWING UNIFORM PRESSURE RISE NEAR SURGE POINT

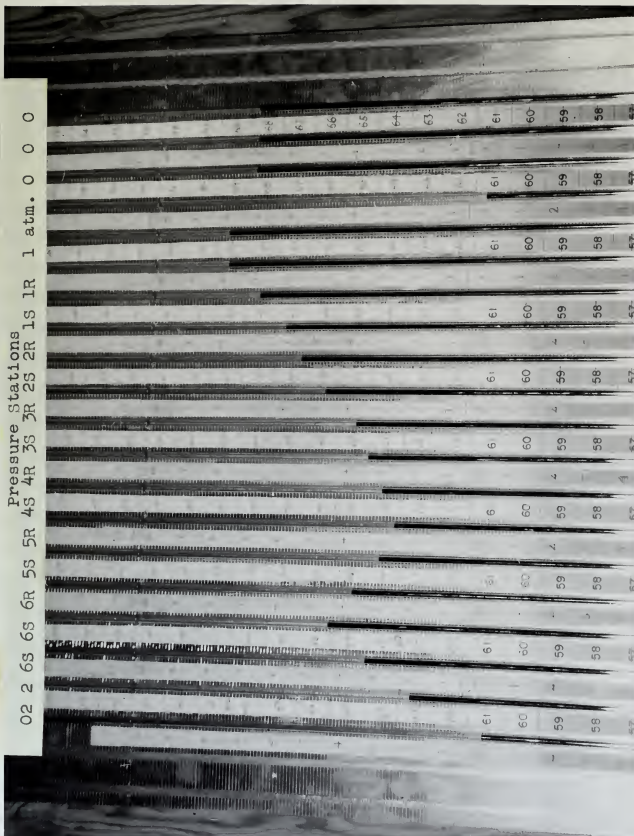


FIGURE 16
 MANOMETER BOARD SHOWING PRESSURE LOSS AT HIGH MASS FLOW

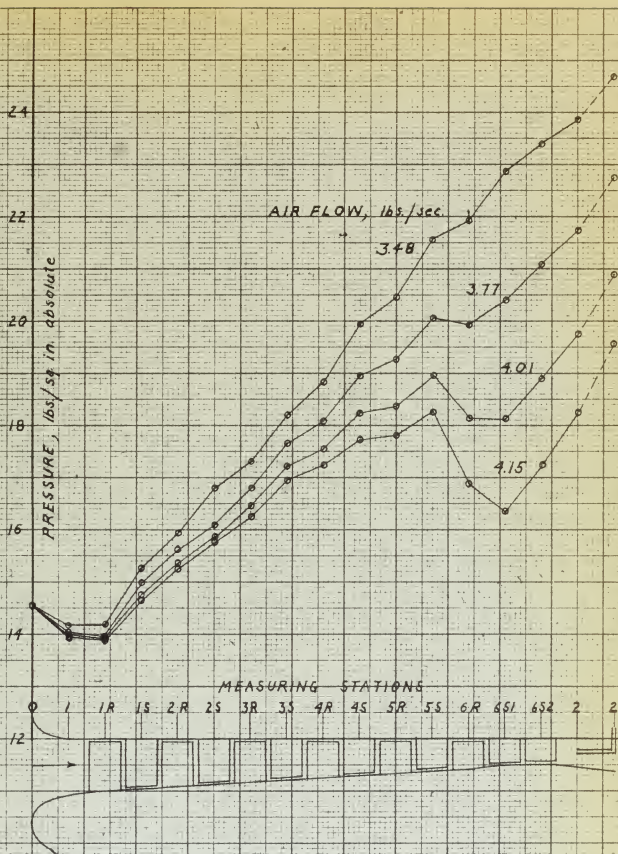


FIG. 17
COMPRESSOR AXIAL PRESSURE
DISTRIBUTION

INLET DENSITY = 0.0726 lbs./cu. ft.
22,000 RPM

COMPRESSOR EFFICIENCY, %

COMPRESSOR PRESSURE RATIO, P_2/P_1

CORRECTED FRACTION RATED AIR FLOW, $\frac{W}{W_0}$

NOMINAL
COMPRESSOR
REYNOLDS
NUMBER

△	175,100
□	162,800
○	126,000
○	115,100

SURGE LIMIT

FIG. 18 (a)
COMPRESSOR PERFORMANCE MAP
NOMINAL COMPRESSOR MACH NUMBER = 0.461

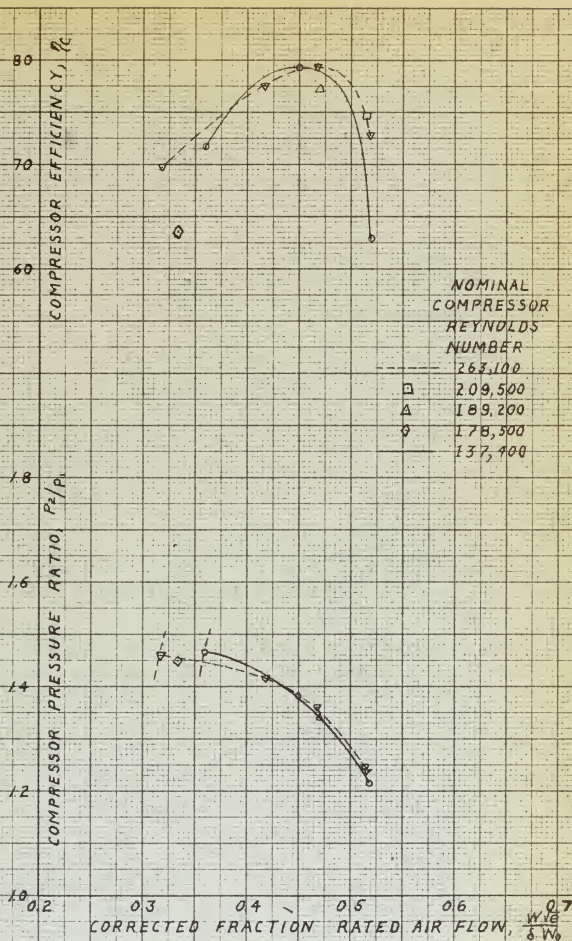


FIG. 18 (b)

COMPRESSOR PERFORMANCE MAP

NOMINAL COMPRESSOR MACH NUMBER = 0.546

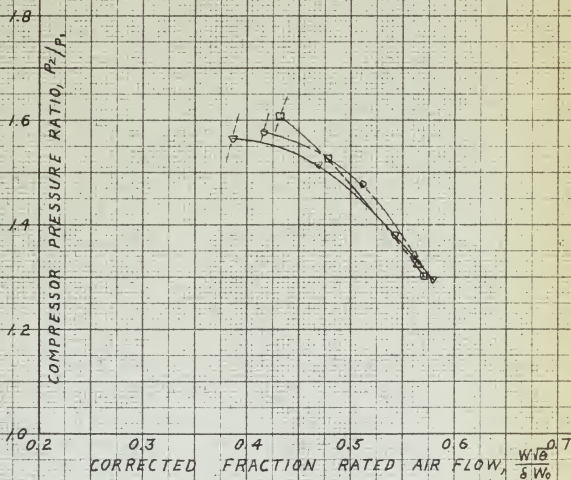
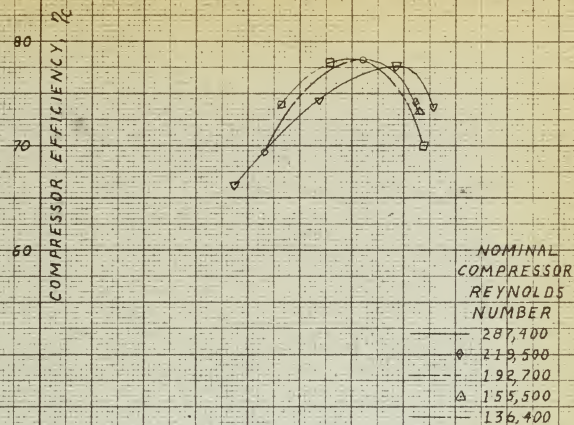


FIG. 18 (c)
 COMPRESSOR PERFORMANCE MAP
 NOMINAL COMPRESSOR MACH NUMBER = 0.605

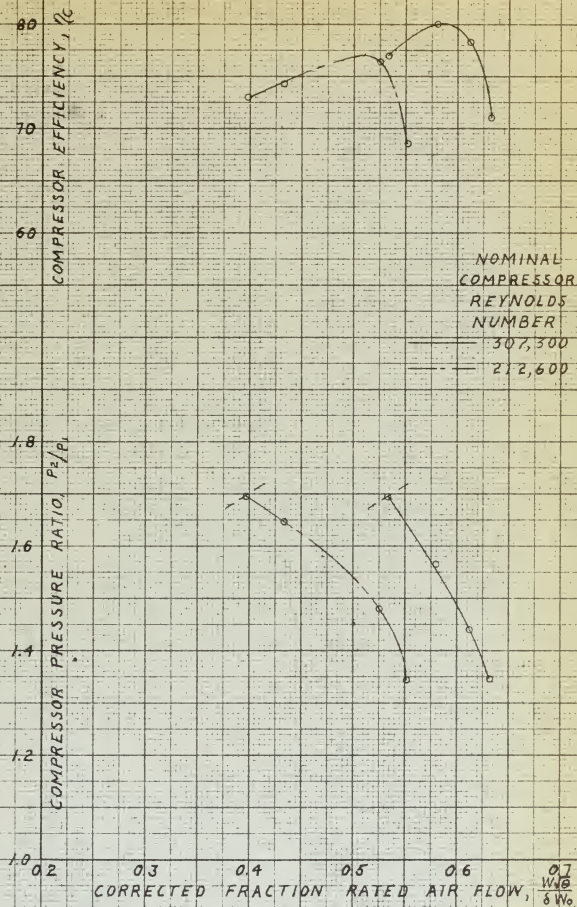


FIG. 18(d)
COMPRESSOR PERFORMANCE MAP
NOMINAL COMPRESSOR MACH NUMBER = 0.658

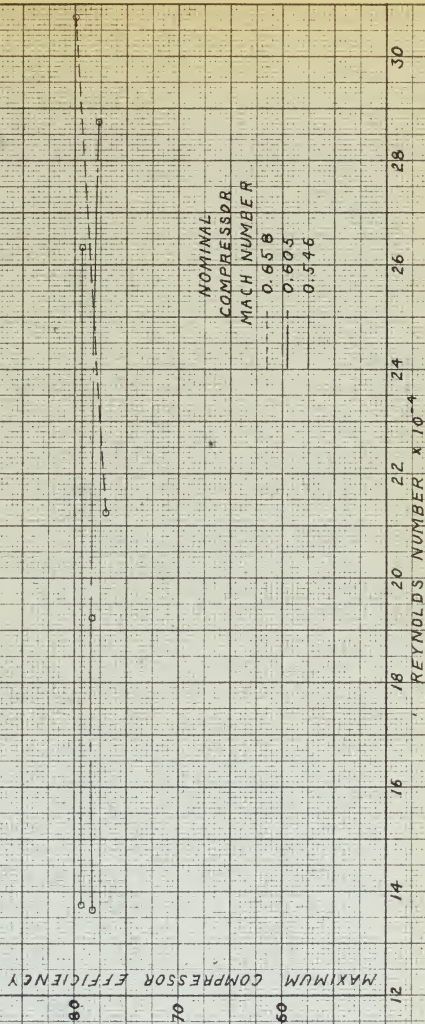


FIG. 19
VARIATION OF MAXIMUM COMPRESSOR EFFICIENCY WITH
REYNOLDS NUMBER

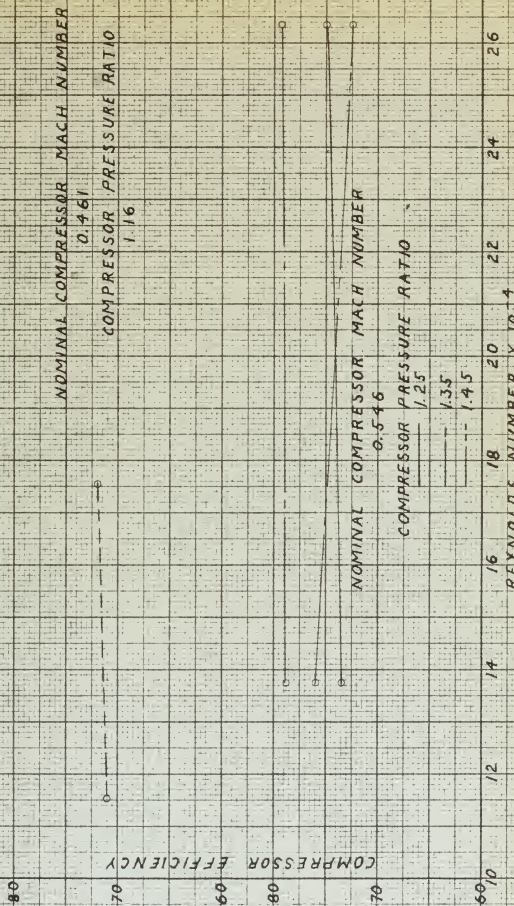


FIG. 20 (a)
 VARIATION OF COMPRESSOR EFFICIENCY WITH
 REYNOLDS NUMBER

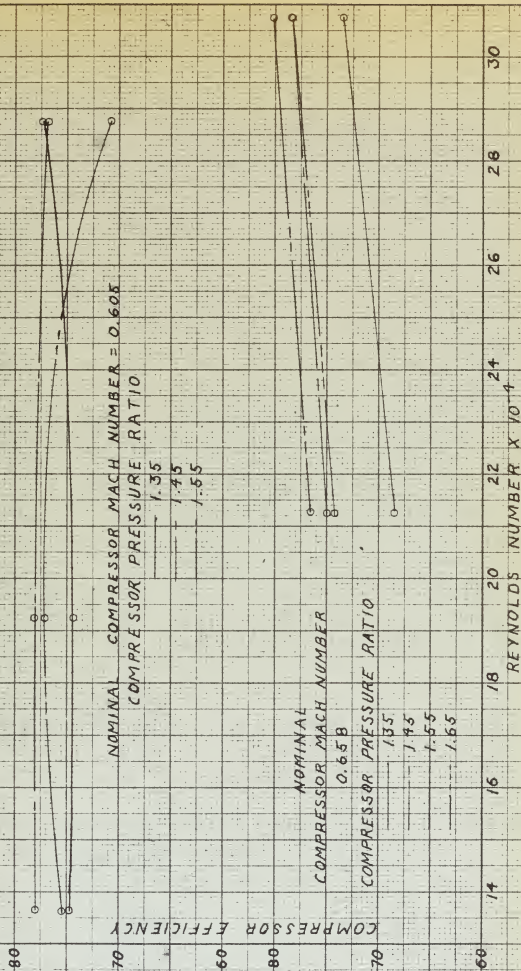


FIG. 20(b)
VARIATION OF COMPRESSOR EFFICIENCY WITH
REYNOLDS NUMBER

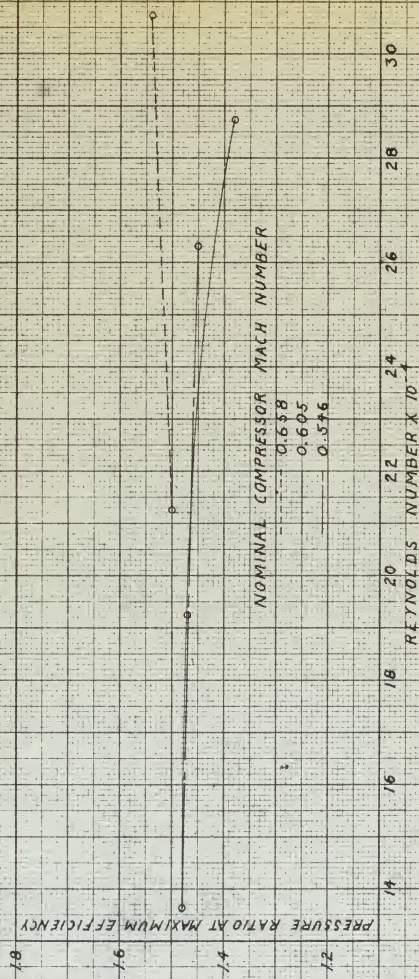


FIG. 21
 VARIATION OF PRESSURE RATIO FOR MAXIMUM
 EFFICIENCY
 WITH REYNOLDS NUMBER

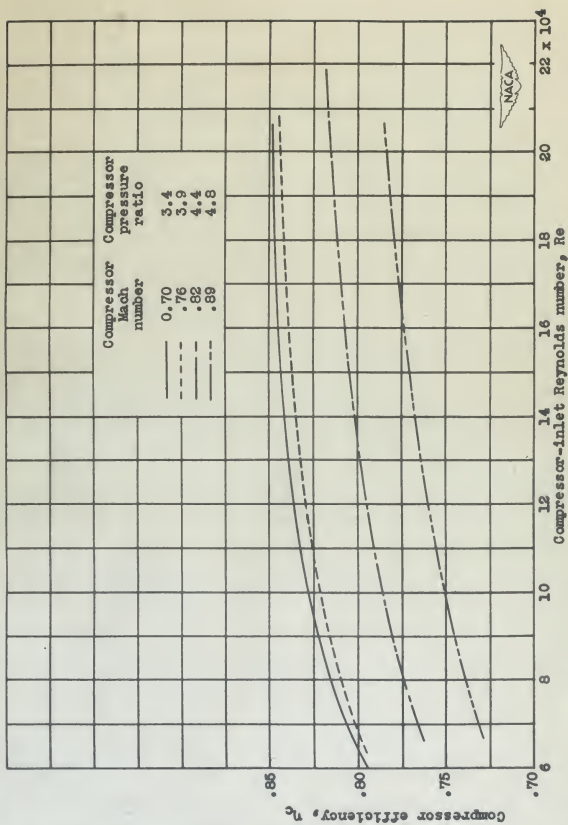


Figure 22. - Effect of compressor-inlet Reynolds number on compressor efficiency.

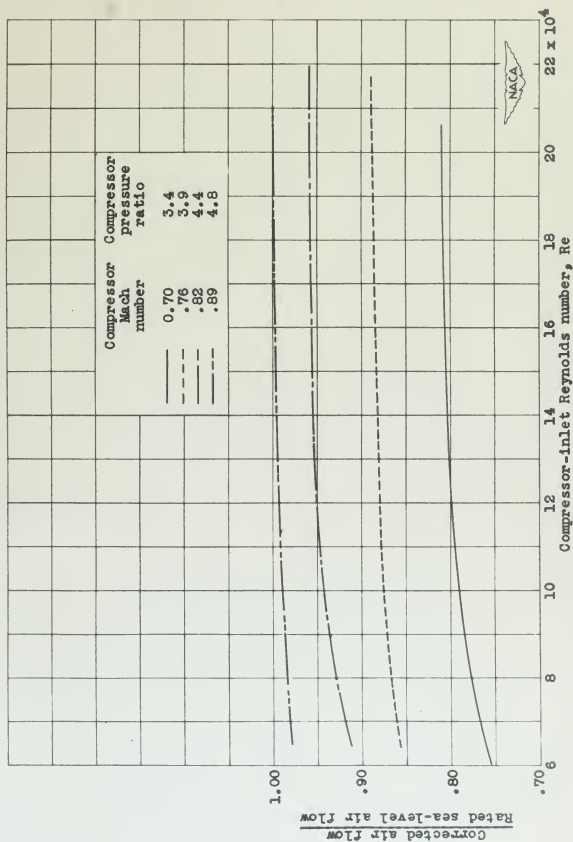


Figure 23. - Effect of compressor-inlet Reynolds number on fraction of rated sea-level air flow.

Thesis

H202 Hansen

17315

An investigation of the performance of an axial flow compressor with emphasis on the effect of Reynolds number.

DATE

ISSUED TO

Thesis

H202

Hansen

17315

An investigation of the performance of an axial flow compressor with emphasis on the effect of Reynolds number.

Library

U. S. Naval Postgraduate School
Monterey, California



thesH202

An investigation of the performance of a



3 2768 002 07650 7

DUDLEY KNOX LIBRARY